Lincoln University Digital Dissertation

Universität für Bodenkultur Wien
University of Natural Resources and Life Sciences, Vienna

Department of Water, Atmosphere and Environment
Institute of Sanitary Engineering and Water Pollution Control

VERIFICATION OF THE IMPLEMENTATION OF CWM1 IN THE HYDRUS WETLAND MODULE

A thesis submitted in partial fulfilment
of the requirements for the Degree of

International Master for
Natural Resources Management and Ecological Engineering

at

University of Natural Resources and Life Sciences, Vienna, Austria and
Lincoln University, Lincoln, New Zealand

by

TAMÁS GÁBOR PÁLFY

Supervisor:	Dr. Günter Langergraber, Priv.-Doz. University of Natural Resources and Life Sciences, Vienna
Co-Supervisor:	Dr. Sam Carrick Landcare Research, New Zealand

Reg. no.: 1041612 12.08.2013

Whatungarongaro te tangata toitū whenua.

- As man disappears from sight, the land remains.

Abstract

The Constructed Wetland Model N°1 (CWM1) is a numerical biokinetic model describing microbial transformation and degradation processes in subsurface flow constructed wetlands. In this master thesis the CWM1 implementation in the HYDRUS wetland module was verified using data from previously conducted controlled environment column experiments. These twenty day long batch experiments used synthetic wastewater and three different plant species (*Carex rostrata* Stokes, *Schoenoplectus acutus* Muhl. Ex Bigelow and *Typha latifolia* L.) in addition to unplanted replicates at four different temperatures. The minimum number of adjusted parameters between the sixteen simulated columns was targeted, and it was found that: (1) initial bacterium concentrations, (2) initial adsorbed ammonia nitrogen concentrations, and (3) root oxygen loss rate for each simulation inevitably needed to be set separately. For all other parameters the same values have been used. Some biokinetic parameters had to be adapted during calibration to match measured data. This was required to allow anaerobic, anoxic and aerobic processes to run parallel and explained by the local effect of root zone re-aeration. The simulation results were evaluated by conventional visual and numerical and a new goodness of fit analysis method, deflection analysis. The new method was introduced to compare simulations to measured data with standard deviation. Simulated contaminant concentrations had a very good fit to measured values of NH_4-N and SO_4-S and a reasonable good fit to measured values of COD versus time.

Kurzfassung

Das Constructed Wetland Model N°1 (CWM1) ist ein numerisches Modell das die mikrobiellen Abbau- und Transformationprozesse in bepflanzten Bodenfiltern beschreibt. Die Implementierung von CWM1 im HYDRUS wetland module wurde mit Daten von Säulenversuchen in kontrollierter Umgebung im Rahmen der Masterarbeit verifiziert. Bei diesen Versuchen wurde synthetisches Abwasser mit Säulen (drei unterschiedlichen Pflanzenarten (*Carex rostrata* Stokes, *Schoenoplectus acutus* Muhl. Ex Bigelow und *Typha latifolia* L.) und eine unbepflanzte Säule) bei vier unterschiedlichen Temperaturen im Batchbetrieb gereinigt (Dauer einer Charge: 20 Tage). Ein Ziel der Masterarbeit war einen Parametersatz zu finden, bei dem möglichst wenige Parameter für die sechzehn simulierten Säulenversuche zu ändern sind. Es zeigte sich, dass (1) die Anfangskonzentration der Bakterien, (2) die Anfangskonzentration des adsorbierten Ammonium-Stickstoffs, und (3) die Rate der Geschwindigkeit des Sauerstoffverlustes der Wurzeln für alle Säulen geändert werden müssen. Für alle anderen Parameter wurden dieselben Werte verwendet. Einige Parameter des biokinetischen Modells wurden während der Kalibration angepasst. Dadurch wurde es erst möglich zu simulieren, dass anaerobe, anoxische und aerobe Prozessen gleichzeitig ablaufen können. Das ist nötig, um die durch den Sauerstoffeintrag verursachten lokalen Effekte in Wurzelnähe zu simulieren. Die Simulationsergebnisse wurden durch konventionelle visuelle und numerische Vergleiche mit den Messdaten verglichen. Um die Standardabweichung der Messdaten mit zu berücksichtigen, wurde eine die Methode "***deflection analysis***" entwickelt. Zusammenfassend gesagt waren simulierte Schadstoffkonzentrationen in einem sehr guter Übereinstimmung mit gemessenen NH_4-N und SO_4-S Konzentrationen und in guter Übereinstimmung mit gemessenen CSB Konzentrationen.

Table of Contents

List of Tables

List of Figures

Abbreviations

ASM: **A**ctivated **S**ludge **M**odel (Henze et al., 2000).

C_{INI}: Initial concentration of a model component C, e.g. bacterium or contaminant.

cRoot: If water uptake is considered then *cRoot* is automatically used for the maximum concentration of water removed from the flow region by root water uptake. When a zero is specified, all solute is left behind in the soil and only a solute-free solution is being taken up. When the concentration is lower than *cRoot*, all solute is taken up.

CW: **C**onstructed **w**etland

CW2D: **C**onstructed **W**etland **2D** (biokinetic model)

CWM1: **C**onstructed **W**etland **M**odel N°**1** (biokinetic model)

DEF: Deflection, see page 25

DO: **D**issolved **o**xygen

E_j: coefficient of efficiency (Ahnert et al., 2007) with exponent j

hCritA: The minimum allowed pressure head at the soil surface.

HF: **H**orizontal **f**low

MAG: Magnitude of deflection, see page 25

R^2: Coefficient of determination

SD: **S**tandard **d**eviation

TON: **T**otal **O**rganic **N**itrogen

VF: **V**ertical **f**low

Components of CWM1

SA: Fermentation products as acetate

SF: Fermentable, readily biodegradable soluble COD

SH2S: Dihydrogensulphide sulphur

SI: Inert soluble COD

SNH: Ammonium and ammonia nitrogen

SNO: Nitrate and nitrite nitrogen

SO: Dissolved oxygen, O2

SSF: **S**ub**s**urface **f**low

SSO4: Sulphate sulphure

XA: Autotrophic nitrifying bacteria

XAMB: Acetotrophic methanogenic bacteria

XASRB: Acetotrophic sulphate reducing bacteria

XFB: Fermenting bacteria

XH: Heterotrophic bacteria

XI: Inert particulate COD

XS: Slowly biodegradable particulate COD

XSOB: Sulphide oxidizing bacteria

1 Introduction and Objectives

In the recent years, constructed wetlands (CWs) have become increasingly important in several regions of the world. More efficient experimental designs have been achieved, which together with operational experiences and models, have served as guidance tools for research and development (Kadlec and Wallace, 2009). This new knowledge and understanding of constructed wetlands has led to the development of numerical models similar to Activated Sludge Models (ASMs) (Henze et al., 2000), designed to simulate biological treatment processes in subsurface flow wetlands. Two such biokinetic model formulations are included in the Wetland Module of the HYDRUS Software (PC Progress s.r.o, ©) as the only commercially available tools (Langergraber and Šimůnek, 2011, 2012). These are CW2D (Langergraber and Šimůnek, 2005) and CWM1 (Langergraber et al., 2009b), two relatively young tools which aim to lead to similarly important achievements as ASMs did in their own discipline through their ongoing development and use.

To help the development, the implementation of a numerical biokinetic model, Constructed Wetland Model N°1 (CWM1) in the HYDRUS Wetland Module was selected for verification. A way to verify the functionality of a computer-based numerical model is to pair it to real-physical experiments. The more is known about these experiments, in terms of detailed measured data and the better the conceptual understanding of physical processes driving the experimental outcomes, the better researchers are able to investigate the functionality and issues around modelling predictions. In this point of view the best physical experiment is a physical model, a column microcosm. It is the small-scale representation of a CW with the possibility to control its environment, to operate different setups parallel and to put it under intensive monitoring. It can help to understand the degradation and transformation process of CWs providing insight in these complex systems. If we have the same, known parameters and variables in both the physical experiment and numerical conceptualization, they should provide the same outcomes on which the verification of the numerical model can be based. In this project a physical column experiment was compared with its numerical representation. The two systems should provide the same or similar results and pollutant dynamics if all important parameters match – if they do not, the numerical one may need some conceptual re-thinking and modification. Even the physical experiment setup can be imperfect. Its results are unquestionably real; however, misconceptualization of these results, the processes involved, or inconsistent column setup can lead to a result which is distorted or misinterpreted.

Numerical modelling can provide better understanding of wetland processes and operation needs by providing insight in the functionality and dynamics of the complex system of CWs, just as physical models can. Compared to physical experiments like column microcosms a numerical model can be more flexible and cost and time effective. It

can help to improve physical models as physical models can help to improve numerical models. The overall objective of the master thesis was:

- The verification of the implementation of Constructed Wetland Model N°1 (CWM1) in the HYDRUS Wetland Module by controlled-environment physical column data,

which was accomplished attaining the following specific objectives:

- Interpret the outcomes of a previous work on CWM1 verification by Mburu et al. (2012) and considering any weaknesses of their setup strive to establish a parameter set which fits well the results of columns both unplanted and planted by various plant species at different temperatures
- Define a parameter set with minimum number of parameters that have to be adjusted between different columns and temperatures.

The next chapter, Fundamentals, is providing basic knowledge about constructed wetlands and their importance, putting forth the actual issues which can be targeted by modelling. After pointing out some possibilities in numerical models, tools are demonstrated which are presently in use or were recently developed. CWM1 is discussed in-depth, including its formulation and its alternative implementations.

The description of the physical column experiments and the process of model parameterization and goodness of fit analysis are included in the chapter Materials and Methods. Measured column experiment data was used for the verification in which columns were set up unplanted and with different plant species and experiments were carried out at different temperatures in a controlled greenhouse environment. The microcosms were batch-operated for twenty days each using synthetic wastewater with known constituents (Allen et al., 2002). These columns are good subjects for model verification because of the uniformity of their controlled environment and wastewater quality, the batch operation, the wide temperature range and the different plant species planted. The chapter enumerates the main setup steps to establish a standard set of parameters, after which only initial concentrations of bacteria and sorbed ammonia and root oxygen loss representing re-aeration had to be calibrated.

The Results and Discussion chapter includes the calibrated parameters, visual and numerical goodness of fit evaluation and diagrams of pollutant concentrations in all forty-eight columns. The weakest results were identified and analysed. Some suggestions were made for the improvement of the physical experiment setup which can help to build column for model verification and thus can help to increase the reliability of both the physical and numerical models.

The chapter Conclusions contains the interpretation of the results and summarizes the main findings of the master thesis. The chapter Outlook enumerates some of the on-going research and ideas which might be significant in the future of CW modelling.

2 Fundamentals

2.1 Subsurface flow constructed wetlands and their research

2.1.1 The concept of subsurface flow constructed wetlands and their use

Constructed wetlands (CW) are state-of-the-art extensive solutions for wastewater treatment. The wide range of their application includes (Campbell and Ogden, 1999; Kadlec and Wallace, 2009):

- Single households or dwellings
- Municipal wastewater, usually for smaller communities
- Extension of existing facilities
- Industrial, mining and agricultural wastewaters and wastewaters with special characteristics such as e.g. landfill leachate
- Stormwater runoff and combined sewer overflow

CWs are solar powered and/or powered by the energy stored in the contaminants. Due to self-regulating processes, treatment wetlands are capable of tackling a wide range of pollutants at low maintenance and energy costs (Campbell and Ogden, 1999; Kadlec and Wallace, 2009). The quality of the effluent is comparable to secondary or tertiary effluents of other treatment technologies and they have a wide range of use. Advantages of CW include location flexibility, no alteration of natural wetlands, low or normal construction costs, simple and cheap operation and maintenance, process stability under varying conditions of the environment, as well as they are aesthetic and possible habitats for wildlife (Tanner and Kloostermann 1997, Campbell and Ogden 1999, Polprasert 2006). Langergraber and Šimůnek (2012) build a good concise general description of them:

'CWs are engineered treatment systems that optimize treatment processes found in natural environments and are therefore considered to be sustainable, environmentally friendly solutions to engineering problems. Processes occurring in CWs are very complex, and include a large number of simultaneously active physical, chemical and biological processes that mutually influence each other.'

Extraneous environmental effects will have varying significance on treatment processes at different locations making CWs even more complicated to design and operate. For example, temperature of air, soil temperatures, humidity, rainfall extremities and sunshine hours might have to be included to design criteria.

We can distinguish two main categories of wetlands used for wastewater treatment. These are surface flow or free water surface (FWS) and subsurface flow (SSF) systems. We can make further categorization according to vegetation and flow direction, as shown on Table 1. The focus of this master thesis is SSF CW modelling.

Table 1: Categories of wetlands used for wastewater treatment (after Kadlec and Wallace, 2009).

Treatment wetlands				
Surface flow			Subsurface flow	
Emergent plants	Floating plants	Submerged plants	Horizontal flow (HF)	Vertical flow (VF)

In Polprasert (2006) SSF CWs are considered as rather anaerobic systems with lateral flow. This description fits well with HF systems but VF systems have different characteristics in terms of loading, saturation conditions and aeration. The loading of the beds is intermittent, resulting in varying saturated and unsaturated states of the filter media. This helps restore aerobic conditions and thus makes feasible higher BOD and ammonium nitrogen removal (Reed et al. 2006). The common feature of the design of SSF CWs is the water stays below the surface. The media supports bacterial and biofilm growth and also physical and chemical cleansing processes on the surface of the soil particles, which is supported by plant uptake, root oxygen and exudate transfer. Beds are isolated via natural or synthetic materials on the bottom and sides. The structural difference between HF and VF subsurface systems is represented by Figure 1.

Figure 1: Horizontal flow (left) and vertical flow (right) subsurface flow constructed wetlands (SSWM, 2013).

2.1.2 Open and returning questions of research

The research and development of SSF CWs is active nowadays and targets better design for higher treatment efficiency, better scale of economy, alternative application fields and improved design tools. Without aiming at completeness, the following questions and research topics are actively discussed by many journal publications:

- The effect of different plant species on treatment efficiency due to root oxygen loss and exudates (e.g. Allen et al., 2002; Taylor et al., 2011)
- Applicability of constructed wetlands in cold climate (e.g. Allen et al., 2002; Langergraber et al., 2011a)
- Treatment efficiency as a function of seasons (e.g. Allen et al., 2002; Stein et al., 2007; Taylor et al., 2011)

- Improvement of and driving forces behind nitrogen removal (e.g. McBride and Tanner, 2000; Langergraber et al., 2011b; Tanner et al., 2012)
- Application possibilities for the removal of special contaminants like e.g. heavy metals, micropollutants and PAHs and application beyond municipal wastewater (e.g. Grove and Stein, 2005; Stein et al., 2007)
- Lifecycle estimation and planning – deposition and clogging processes (e.g. Brovelli et al., 2009b)
- Modelling solutions as a tool for R&D and design (e.g. Brovelli et al., 2009a,b; Toscano et al., 2009; Langergraber and Šimůnek, 2012)

2.2 Options for subsurface flow constructed wetland modelling

Due to their complexity SSF CWs were often considered as black boxes and for this reason Austrian (ÖNORM B 2505, 2009), and New Zealand (Tanner and Kloostermann 1997, Tanner et al. 2010, Tanner et al. 2011) standards and guidelines are based on rules of thumb using a specific surface area requirement or some simple first-order decay models. In Langergraber et al. (2009a), three options for models were discussed: simple transport and first order decay models, complex mechanistic models and a simplified model that has been developed for retention soil filter designing purposes.

Simple transport and first-order decay models are based on fundamental laws governing water flow and solute transport. By making assumptions on system geometry and defining boundaries, the governing equations can be reduced to a set of closed-form formulas which are often useful to evaluate water flow and transport of inert solutes including the estimation of residence time, degree of mixing and hydrodynamic dispersivity. The drawbacks of the method are its limited validity to situations where the underlying assumptions hold and the simplification to one dimensional behaviour where the effects of dispersion, heterogeneity and dead zones are lumped together in the hydrodynamic dispersivity term. These can cause a significant error in the calculations, and, for example, errors of the effective residence time will be transmitted to the expected degradation efficiency (Langergraber et al. 2009a).

The mentioned Austrian and New Zealand guidelines might be satisfactory but to improve design criterion for site-specific issues, for optimized treatment efficiency and better scales of economy, a better understanding of these systems is required. The main objective of the numerical SSF CW (and also CW in general) modelling is defined in Langergraber and Šimunek (2012) based on the findings of Langergraber (2008, 2011):

'… to obtain a better understanding of governing biological and chemical transformation and degradation processes, to provide insights into these "black box" systems, and to evaluate and improve existing design criteria."

Langergraber (2011) enumerates three numerical computational tools capable of constructed wetland pollutant removal modelling relying on CWM1: the HYDRUS wetland module, PHWAT and RETRASO. Furthermore, other tools related to subsurface

flow and transformation processes like groundwater remediation and organic matter removal and oxygen transport are listed because of their close relation. AQUASIM has an implementation of CWM1 with which it can be added to these as a fourth tool (Mburu et al., 2012). Langergraber and Šimůnek (2012) specify sub-models that a complete SSF CW model includes:

1. The model describing water flow in porous media,
2. The transport model including diffusion, dispersion and sorption processes
3. The biokinetic model of biochemical transformation and degradation processes
4. The plant model describing growth, decay, decomposition, nutrient uptake and root oxygen release
5. The clogging model, which has to include the transport and deposition of particulate matter and biological growth which can reduce conductivity of the porous media.

Langergraber et al. (2009a) cover a third type of models, a simplified reaction model of CWs treating combined sewer overflows (CSOs) known as retention soil filters. Meyer (2011) concluded that CSO treatment modelling in CWs requires a reasonable balance between detailed description and practicable handling to optimize design and operation requirements. The use of a complex numerical tool had been shown unpractical for long-term simulations with sewer-system models. Their work is a good example that complexity is not necessarily directly proportional to practicability and also how much can be gained for design purposes from the simplification of a tool.

2.3 Present and short historical overview

The present situation of process-based SSF CW modelling is evaluated by Langergraber and Šimůnek (2012) as follows:

'A number of process-based numerical models for subsurface flow (SSF) CWs have been developed during the last few years. However, most of them are either in a rather early stage of development or are available only in-house. The HYDRUS wetland module is the only implementation of a CW model that is currently publicly available.'

Due to their complexity, CWs were considered as black boxes for a long while and less research was done targeting the better understanding of contaminant removal processes (Kadlec and Wallace, 2009, Langergraber and Šimůnek, 2012).

Langergraber and Šimůnek (2012) pointed out that during the last decade several models have been developed by collecting numerous works in the topic of numerical modelling of SSF CWs and concluded there had been a wide interest in the understanding of the complexity of constructed wetland systems including the modelling of those. However, the research and the development of such models reaches back much further than the last decade as it was not started directly with CWs but it has obtained a lot from experience with a related and older area of science, the activated sludge modelling (Henze et al., 2000). The development of the first ASM which can be considered as forefather of the structure and notation system of many biokinetic models started in 1982 and was

publicised in 1987. The targeted contaminants and biological processes treating wastewater are similar in the case of conventional wastewater treatment and constructed wetlands (see e.g. Kadlec and Wallace, 2009: 267) therefore ASMs and CWM1 have similar structure, components and notation.

CWM1 (Langergraber et al., 2009b) was developed to describe biokinetic transformation processes of organic matter, nitrogen and sulphur in SSF CWs, including all relevant aerobic, anoxic and anaerobic treatment processes for these contaminants. It is a complex tool for modelling SSF biokinetics; however, it needs to be integrated with other models as it represents a part of a complete SSF CW model. Because of the necessity of other submodels CWM1 was not implemented as a standalone tool but uses other features programmed into or included as standard in environmental modelling software (see 2.4.2 Other implementations of CWM1). For example, many submodels of HYDRUS are fundamental to model SSF CW and are developing together or parallel with CWM1 to target special and not exclusively CW related issues like root re-aeration, preferential flow and transport and deposition of particulate matter.

2.4 Constructed Wetland Model N°1 (CWM1)

2.4.1 CWM1 in the HYDRUS Wetland Module

The software package of HYDRUS is a tool for simulating two- and three dimensional variably-saturated water flow, heat and solute transport in the porous media involved in sequential first-order decay reactions. The software solves numerically the Richard's equation for saturated and unsaturated water flow and the convection-dispersion equation for heat and solute transport. There is a sink term in the flow equation representing root water uptake. The solute transport equations consider convective-dispersive transport in the solute phase, diffusion in the gaseous phase and non-linear non-equilibrium reactions between those two (Šimůnek et al., 2011).

The second version of the HYDRUS wetland module (Langergraber and Šimůnek, 2012) includes two biokinetic model formulations for the simulation of reactive transport processes of SSF CWs: CW2D (Langergraber and Šimůnek, 2005) and CWM1 (Langergraber et al., 2009b). They were developed to model SSF CWs treating municipal wastewater but were used to simulate combined sewer overflow, agricultural runoff and tertiary effluents as well (Langergraber and Šimůnek, 2012, Pálfy and Langergraber, 2013). The HYDRUS software package with the wetland module is compared here to a theoretically complete SSF CW model:

1. The model describing water flow in porous media: incorporates saturated and unsaturated flow but can't simulate preferential flow which can have especially great significance in the case of French system (see Albold et al., 2011) because of the cracking in the drying sludge surface (Chazarenc, 2013).
2. The transport model including diffusion, dispersion, adsorption and desorption
3. The biokinetic model of biochemical transformation and degradation processes: two built-in numerical models can be selected – CW2D and CWM1.

4. The plant model describing growth, decay, decomposition, nutrient uptake and root oxygen release: root nutrient uptake and oxygen release are incorporated in a similar way, but growth, decay and decomposition of wetland plants can't be modelled.
5. The clogging model, which has to include the transport and deposition of particulate matter and biological growth reducing conductivity of the porous media: this component is completely missing. It can be used to model the age-related performance decrease (see Brovelli et al. 2009b, Kadlec and Wallace, 2009, Langergraber et al., 2009b).

Only aerobic and anoxic processes are considered in the CW2D biokinetic model and therefore it is not applicable for CWs in which anaerobic processes play a significant role (Langergraber and Šimůnek, 2012). The same conclusion was made during research targeting the applicability of a HF CW in Balf, Hungary for polishing tertiary treated wastewater with casual peak concentrations exceeding legislative thresholds. Simulations were conducted using CW2D and the model was not capable to tackle highest peak organic loads which resulted in anaerobic conditions (Pálfy and Langergraber, 2013).

The implementation of CWM1 in HYDRUS is capable to simulate fixed biomass which is of high importance to obtain realistic treatment efficiency results (Langergraber and Šimůnek, 2012). Langergraber et al. (2009b) intended to provide a widely accepted model of the biochemical processes in SSF CWs by creating CWM1. It is capable of simulating aerobic, anoxic and anaerobic transformation processes of organic, nitrogen and sulphur compounds in wastewater. It is asserted in *ibid.* that:

'CWM1 describes all relevant aerobic, anoxic, and anaerobic biokinetic processes occurring in HF and VF CWs required to predict effluent concentrations of organic matter, nitrogen and, sulphur.'

It is common to use the notation system introduced by the IAWPRC (International Association on Water Pollution Research and Control, the predecessor of IWA) Task Group for biokinetic models. The so-called *Gujer* matrix was named after Willi Gujer, Emeritus Professor ETH Zürich and co-author of the article introducing the first ASM, Activated Sludge Model N°1. The goal of this matrix notation was to create an understandable and standard language for the modelling of activated sludge processes (Henze et al., 2000). Every propagation and metabolic process done by a certain microbial group is described through three important parts of the matrix. The first two are the composition of substrates and products (header) and kinetic rate expression (without header, added after each row). Each growth and decay process is represented by one row of the matrix and is filled with stoichiometric equations of each component. A simple Gujer matrix for heterotrophic aerobic growth and decay is shown in Table 2, modified after Langergraber and Šimůnek (2012) by shading each of the main parts separately.

Table 2: An example of Gujer matrix denoting the biokinetics of and transformation processes caused by the aerobic growth and decay of heterotrophic bacteria (modified after Langergraber and Šimůnek, 2012).

	Heterotrophic biomass mg COD L^{-1}	Substrate mg COD L^{-1}	Dissolved oxygen -mg COD L^{-1}	Composition Kinetic rate expressions Stoichiometry
Component (i)	1	2	3	**Process rate** $_j$
Process (j)	X_{OHO}	S_B	S_{O2}	
1. Growth	1	$-\frac{1}{Y_{OHO}}$	$-\frac{1-Y_{OHO}}{Y_{OHO}}$	$\mu_{OHO,Max}\frac{S_B}{K_{SB,OHO}+S_B}\frac{S_{O2}}{K_{SO2,OHO}+S_{O2}}X_{OHO}$
2. Decay	-1		-1	$b_{OHO}\ X_{OHO}$

Stoichiometric parameters: Y_{OHO} = Heterotrophic yield coefficient

Kinetic parameters: $\mu_{OHO,Max}$ = Maximum heterotrophic growth rate

$K_{SB,OHO}$ = Half-saturation coefficient for substrate

$K_{SO2,OHO}$ = Half-saturation coefficient for oxygen

b_{OHO} = Heterotrophic decay rate

Two modelled processes are described this way representing the activity of heterotrophic bacteria. It is involving three components, the biomass itself and substrate and oxygen consumed during metabolism. Heterotrophs find their energy source in organic carbon which is partly contributing to biomass growth ($1/Y_{OHO}$) and partly oxidized for energy production ($1\text{-}1/Y_{OHO}$, transformed on the chart to $-\frac{1-Y_{OHO}}{Y_{OHO}}$) (Langergraber and Šimůnek, 2012).

In this example, growth depends on the present amount of biomass X_{OHO}, maximum growth rate $\mu_{OHO,Max}$, substrate availability S_B and electron acceptor availability S_{O2}. The latter two are expressed via Monod-type equations, where K_x is the half-saturation coefficient. By switching the numerator to the same K_x constant, it becomes an inhibition coefficient and thus this equation is capable to describe the inhibition characteristics of a certain component. Nutrient, alkalinity and other component dependence can also be modelled this way (Langergraber and Šimůnek, 2012).

Reaction and propagation rates are calculated by multiplying each of the stoichiometric equations by the corresponding process rate equation and results are summed up by compound. For example, the changes in heterotrophic bacteria concentration, as a sum of simultaneous growth and decay can be calculated by Equation 1 (Langergraber and Šimůnek, 2012).

$$r_{x_{OHO}}=\mu_{OHO,max}\frac{S_B}{K_{SB,OHO}+S_B}\frac{S_B}{K_{SO2,OHO}+S_{O2}}X_{OHO}+(-b_{OHO}X_{OHO}) \quad (1)$$

There are sixteen components defined in CWM1 and one non-reactive tracer. It is assumed that all components are soluble, except bacteria which is immobile. Organic nitrogen is modelled as part of the COD. All components are listed in Table 3 which summarizes also in what phase these components can occur in the model. Components that can be defined in both liquid (L) and solid phase (S) can be subjected to adsorption and desorption.

Table 3: The components of CWM1 and the phases they are defined (L = liquid phase and S = solid phase; after Langergraber and Šimůnek, 2012).

	Symbol	Component	Phase
1.	SO	Dissolved oxygen, O_2	L
2.	SF	Fermentable, readily biodegradable soluble COD	L+S
3.	SA	Fermentation products as acetate	L+S
4.	SI	Inert soluble COD	L+S
5.	SNH	Ammonium and ammonia nitrogen	L+S
6.	SNO	Nitrate and nitrite nitrogen	L
7.	SSO4	Sulphate sulphure	L
8.	SH2S	Dihydrogensulphide sulphur	L
9.	XS	Slowly biodegradable particulate COD	L+S
10.	XI	Inert particulate COD	L+S
11.	XH	Heterotrophic bacteria	S
12.	XA	Autotrophic nitrifying bacteria	S
13.	XFB	Fermenting bacteria	S
14.	XAMB	Acetotrophic methanogenic bacteria	S
15.	XASRB	Acetotrophic sulphate reducing bacteria	S
16.	XSOB	Sulphide oxidizing bacteria	S
17.		Non-reactive tracer	L+S

Aerobic, anoxic and anaerobic processes are all considered in CWM1 and modelled based on the activity of six different bacterium groups. These and the transformation processes for which they account for in the model are listed in Table 4.

Table 4: Modelled biokinetic processes in CWM1 (after Langergraber and Šimůnek, 2012).

Heterotrophic bacteria	
1.	Hydrolysis: conversion of XS to SF
2.	Aerobic growth of XH on SF (mineralization of organic matter)
3.	Aerobic growth of XH on SA (mineralization of organic matter)
4.	Anoxic growth of XH on SF (denitrification)
5.	Anoxic growth of XH on SA (denitrification)
6.	Lysis of XH
Autotrophic bacteria	
7.	Aerobic growth of XA on SNH (nitrification)
8.	Lysis of XA
Fermenting bacteria	
9.	Growth of XFB (fermentation)
10.	Lysis of XFB
Acetotrophic methanogenic bacteria	
11.	Growth of XAMB (anaerobic growth on SA
12.	Lysis of XAMB
Acetotrophic sulphate reducing bacteria	
13.	Growth of ASRB (anerobic)
14.	Lysis of XASRB
Sulphide oxidizing bacteria	
15.	Aerobic growth of XSOB on SH2S (oxidation to SSO4)
16.	Anoxic growth of XSOB on SH2S (oxidation to SSO4)
17.	Lysis of XSOB

Additional information can be found in the manual of the wetland module (Langergraber and Šimůnek, 2011) and the technical manual of HYDRUS (Šimůnek et al., 2011).

2.4.2 Other implementations of CWM1

2.4.2.1 PHWAT for SSF CW modelling

Brovelli et al. (2009a) extended the capabilities of a variably density-flow and reactive transport code called PHWAT in order to make it capable to model sand filters and constructed wetlands. They developed additional models to it exploiting its modular structure. With those the toolkit was capable of modelling unsaturated flow by numerically solving the Richard's equation, complex biogeochemical reaction networks including biological transformations based on CWM1 and clogging as a result of biomass growth and the filtration and precipitation of suspended solids. Model calibration had proven extremely difficult due to the strong non-linearity of the mathematical model behind (Langergraber et al. 2009a).

2.4.2.2 CWM1-RETRASO

CWM1 was added into RETRASO by Llorens et al. (2011a,b) based on the two-dimensional finite element tool, RetrasoCodeBright (RCB). RCB is capable of simulating

reactive transport of dissolved and gaseous species for non-isothermal variably saturated flow domains. In Llorens et al. (2011b) a HF bed was simulated without considering attached bacteria (or biofilm). For this reason, unrealistically high constant bacteria concentrations were set for the inflow. Nor the inner distribution profiles neither the associated effects could be modelled. Langergraber and Šimůnek (2012) pointed out how important it can be to include fixed biomass into the model as the availability of substrates and electron acceptors changes through the different parts of the bed, e.g. close to the surface more oxygen is available than at the bottom or, e.g. close to the inflow more substrate is available than at the outflow. The setup in RETRASO resulted in incomplete degradation of organic compounds and high SA concentration at the outflow whereas simulations using fixed biomass resulted in all SA was degraded at about half of the length of the filter bed.

2.4.2.3 CWM1 in AQUASIM

The AQUASIM software was designed for identification and simulation of aquatic systems in laboratory, technical plants and in the nature. AQUASIM allows the user to specify transformation processes, to run simulations based on those and provides tools for sensitivity analysis and parameter estimation (Reichert 1998). Mburu et al. (2012) implemented CWM1 in this tool and added plant model and sorption processes. The model was used to analyse interactions between solute, granular substratum, macrophytes and microorganisms for contaminant transformation and degradation processes in the same batch operated CW microcosms which supported data for the model verification in this master thesis (see chapter 3.1). The SSF CW microcosms were modelled in the mixed reactor component configuration in AQUASIM and the testing of experimental data was performed by sensitivity analysis, parameter estimation and uncertainty analysis.

3 Materials and Methods

3.1 The physical column experiments (Allen et al., 2002)

This subchapter contains the description of a physical model experiment series done by an expert group at Montana State University. The setup and the outcomes of these experiments were published by Allen et al. (2002), more detailed results of measurements were obtained from Mburu (2013) and used for the verification of CWM1.

The greenhouse experiment used column-shaped constructed wetland microcosms (often referred simply as 'columns'). The experiment took place in Bozeman, Montana (N 45°40' W 111°03', at 1490 m elev.) and lasted for about two years. A series of 20-day long batch operations was conducted using synthetic wastewater with known constituents. Temperatures ranged from 4°C to 24°C with a 4°C step between each batch but for this master thesis only the columns with temperatures ranging from 12°C to 24°C were modelled. Artificial lighting was not used, the cumulative daily net solar radiation ranged from 1 to 8 MJ m^{-2} day^{-1} representing about 25% of locally measured values because a fabric light filter was employed to improve the control over the temperature. Relative humidity ranged from 30 to 70% with no seasonal pattern. The control of the temperature and seasonal light pattern supported a robust plant growth and triggered seasonal cycles of plant activity.

Eight replicates were created for each of the unplanted column and of the three planted ones which were potted by beaked sedge (*Carex rostrata* Stokes), hardstem bulrush (*Schoenoplectus acutus* Muhl. Ex Bigelow) and broadleaf cattail (*Typha latifolia* L.). From herein these columns are referred to as unplanted, *Carex*, *Schoenoplectus* and *Typha*. Each of them was made of a polyvinyl chloride (PVC) pipe with 60 cm height and 20 cm diameter filled to a depth of 50 cm. Alluvial pea gravel (0.3-1.3 mm in diameter) of igneous and metamorphic origin was used as filter material with a porosity of 0.27 and a pore volume of about 4.3 litres per column. Three access tubes were installed with an opening at the depth of 5, 15 and 30 cm below the filter media surface and they were equipped with platinum redox electrodes. Evapotranspiration losses were replenished with greenhouse-temperature de-chlorinated tap water added to the bottom of column. Evaporation losses were 0.7 L day^{-1} per column at 24°C and about 0.4 L day^{-1} per column at 4°C. Figure 2 is a photo of the columns taken during the experiment.

Figure 2: The columns and water replenishment system at MSU (Stein, 2012).

The difference of evapotranspiration losses between different plant species was not measured. The significance of dissolved oxygen (DO) inputs through evapotranspiration loss replenishment was assumed to be low. Saturated DO concentrations were assumed for the estimation meaning 5-6 mg O_2 day^{-1} per column, representing about 1% of the total COD content of the batch per day. Measured experiments began after plants had been grown to reasonable size on nutrient solutions and later on synthetic wastewater. Figure 3 shows a scheme of the cross-section of a planted column.

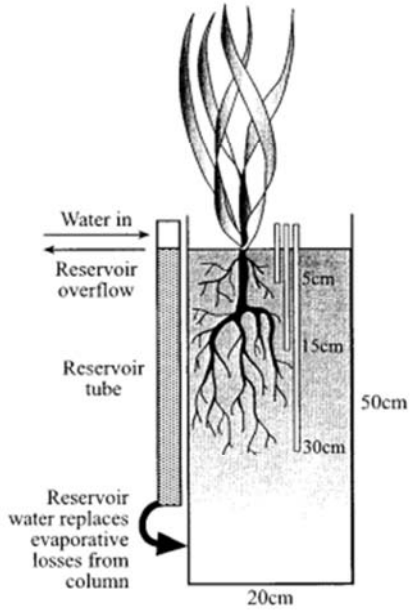

Figure 3: Schematic of the modelled columns and water replenishment system (Allen et al., 2002).

The synthetic wastewater imitated secondary domestic effluent and was mixed from sucrose, hydrolysed meat protein, inorganic nutrients and metal salts. Mean influent concentrations are summarized in Table 5. A more detailed data sheet was available for simulations provided by Mburu (2013) which can be found on Annex IV: DVD.

Table 5: Mean contaminant concentrations in the synthetic wastewater used in the physical experiments (Allen et al., 2002)

Parameter	Contentration
COD	470 mg L^{-1}
Total N	44 mg L^{-1}
Amino-N	27 mg L^{-1}
NH_4-N	17 mg L^{-1}
SO_4-S	14 mg L^{-1}
PO_4-P	8 mg L^{-1}

Columns were gravity drained and filled with synthetic wastewater three days prior to incubations, and again at the beginning of each incubation. Dilution of the incubation wastewater by residual pore water was determined by a bromide tracer to be $\leq 5\%$. Solution samples were collected several times in the first two days of each incubation but the data used for the computer simulations was measured directly after filling and after one, three, six, nine, fourteen and twenty days. The results of these physical experiments were used as a basis of comparison to simulation results.

3.2 Description of model setup

3.2.1 Data sources for model setup

The model was parameterized for the first simulations based on the descriptions of Allen et al. (2002) and some of the results of Mburu et al. (2012), followed by parameter adjustments for a better fit and explainable parameters and results. In some cases no data was available to set certain parameters exactly. Rough estimations were made based on similarities to other experiments or materials discussed in other works including Henze et al. (2000), Langergraber (2001), Salvato et al. (2003) and Kadlec and Wallace (2009).

3.2.2 Time and domain settings

Short time steps are important to minimize the numerical errors of the calculations. Minimum time step was $3x10^{-6}$ d, the maximum 10^{-1} d and the initial 10^{-5} d. The duration of one calculation was about twenty to forty-five minutes. Output information was exported six times on the first day, and thereafter daily which includes the time of all physical measurements.

The columns were modelled in a 10 cm x 50 cm 2D axisymmetric vertical flow domain representing the radius by the height of the physical column, respectively (Figure 4). Simulated processes included water flow, solute and heat transport and root water uptake. Water flow had to be modelled because evapotranspiration losses were compensated at the bottom of the column. Root water uptake was modelled in the

unplanted control column as well, because the parameter defining physical re-aeration did not trigger any oxygen input to the system.

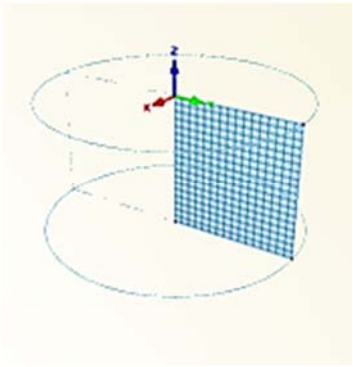

Figure 4: 2D axysimmetrical vertical flow domain used for the simulations (source: HYDRUS user interface).

The domain was represented via a finite element mesh consisting of 31 rows and 21 columns (651 elements). The top boundary was set to be atmospheric for modelling evapotranspiration and the two nodes at the bottom corner on the left side were set as constant head boundary, responsible for the replenishment of evapotranspiration losses. Other boundaries were set to no flux. Figure 5 compares the simulated 2D domain mesh and its boundary conditions with the setup of physical experiments.

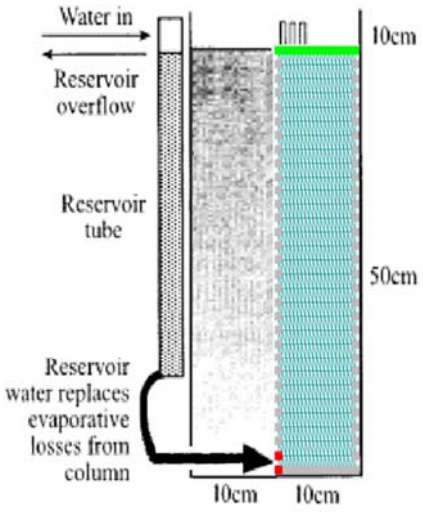

Figure 5: Comparison of the simulated domain mesh and its boundary conditions with the setup of physical experiments. Red: constant head boundary, green: atmospheric boundary, grey: no flux boundary (modified after Allen et al., 2002)

Soil hydraulic parameters were set based on measured and estimated data. Sand was selected from the soil catalogue of HYDRUS and porosity and hydraulic conductivity were changed. The parameters of the water retention function had less significance as the column had been water saturated during all the experiments. The pea gravel used as microcosm media had a measured porosity of 0.27 (Allen et al., 2002) but no hydraulic conductivity data was given. It might be unimportant for the physical experiments but to be

able to simulate the physical setup precisely an exact value would have been helpful instead of estimation. Tap water was injected at the bottom of each column to compensate evapotranspiration losses. Losses were about 0.7 litres per day in the case of 24°C planted columns, making out 14 litres in one batch. This means replacement of 8.26 cm depth of water in the porous media of a column per day significantly effecting dispersion. The conductivity of pea gravel was set to 172,800 cm day^{-1} which is within the range given by Salvato et al. (2003) for gravel media in general.

Filter material and root distribution were set homogenously in all cases. Root distribution was concentrated to the upper half of the physical *Typha* column (see Annex I: Root distribution at the end of the physical experiments), but for the simulations high dispersion coefficients were used so this should not have any implications. Observation nodes were set up in the middle of the model space, at depths of 5, 10 and 30 cm identically to the physical experiment. The observation node at 10 cm was used for result evaluation because also in the physical experiments only the 10 cm-deep observation tube was used for sampling (Allen et al, 2002).

3.2.3 Initial conditions

Initial conditions were fitted to the physical experiment setup described by Allen et al (2002, see chapter 3.1). Estimations were made for initial conditions for which no measured data was available such e.g. initial DO concentration, bacterium concentrations. Fractionation was linked to initial concentration setup because the initial COD concentration had to be divided between SA, SF, SI and XS.

The domain was water saturated and the pressure head was set to be equally distributed with depth. Initial sorbed ammonium concentrations were set after Mburu et al. (2012) but were modified later in all instances. Initial dissolved oxygen concentration was not taken over from their work where the simulations were started with saturated concentrations. Distilled water should not contain any DO, however because the mixing process of the synthetic contaminants might had involved exposure to air initial DO concentrations were set to 1 mg L^{-1}. The low initial DO content is well represented by the measured sulphate concentrations as it starts to drop almost immediately in all cases which could not happen at high or saturated oxygen levels.

Nitrite and nitrate nitrogen, dihydrogen-sulphide sulphur and inert particulate COD concentrations were set to zero, other initial contaminant concentrations were set after measured data. Initial bacterium concentrations ranged on a wide scale of 0.02-5.48 µg g^{-1}. Initial adsorbed SNH concentrations were estimated and changed until a good fit to measured concentrations were achieved. Final values of initial conditions are summarized in Annex III: Model parameters.

3.2.4 Fractionation of COD and organic nitrogen

The initial COD concentration was proportionated between the different fractions of SA, SF, SI, and XS using the recommendations of Mburu et al. (2012) which is the slightly modified version of the recommendations in the ASM models as no particulate organic particles were present in the synthetic wastewater. Therefore XI was set to zero. SF was estimated to be 25%, SA 10%, SI 4% and XS 61% of the total COD (Mburu et al., 2012).

Organic nitrogen is considered in CWM1 as part of the COD (Langergraber et al., 2009b) so it was allocated to different fractions of COD composition. Composition parameters of SF and SI were used as given by Langergraber et al. (2009b; 0.03 and 0.01 g N g^{-1} COD, representing about 3.5 mg L^{-1} and 0.2 mg L^{-1} N, respectively) and the rest of organic nitrogen was allocated as part of XS by increasing its nitrogen content from the standard value of 0.04 g N g^{-1} COD to about 0.084 g N g^{-1} COD, representing about 23.3 mg L^{-1} depending on the actual total COD concentration in the synthetic wastewater which had slight variations between batches of different temperatures. Exact values for all experiments can be found in Annex III: Model parameters. Equation 2 was used to calculate the composition parameter of XS.

$$i_{N,XS} = \frac{TON - i_{N,SF} \times SF - i_{N,SA} \times SA}{XS} \quad (2)$$

where $i_{N,x}$ is the nitrogen content of the COD species $_x$ [g N per g COD_x] and TON is the concentration of total organic nitrogen, 27 mg L^{-1}.

3.2.5 Early-stage transport, root model and biokinetics setup

Transport, root model and biokinetic parameters were adopted from Mburu et al. (2012) and were used as a starting point for the simulations involving the substitution of many standard values. Unit conversions were made where it was necessary to match the input format of HYDRUS, e.g. some adsorption coefficients and initial bacterium concentrations. The bulk density of the filter material was estimated to be 1.79 kg per m^3 (AquaCalc, 2013). Dispersion and diffusion coefficients were set as given by Langergraber and Šimůnek (2011). Dispersion had to be significantly increased during parameter adjustment.

To match the physical model setup a constant head boundary was set at two outer nodes near to the bottom of the column, at 48.33 cm and at 50 cm. These were responsible to balance out evapotranspiration losses by injecting water when pressure head reached a critical value at the top layer. The trigger parameter hCritA was set to -0.01 cm in order to keep the column water saturated all the time. Adding tap water at the bottom to balance evapotranspiration losses as described by Allen et al. (2002) resulted in a strongly diluted layer of solute expanding upwards in time against a shrinking, more and more concentrated layer at the upper part when using the dispersion coefficients used by Langergraber (2001). High longitudinal and transversal dispersion coefficients had to be used to ensure homogenous concentrations through mixing.

Root functions had to be added also to unplanted microcosms because the parameter defining physical re-aeration (parameter "Rate O_2") only describes oxygen exchange between gaseous and liquid phase in unsaturated conditions. There were no unsaturated zones in the domain where gas exchange can happen between the liquid and gaseous phase. This was overcame by setting root distribution in the entire column equally which was satisfactory because the physical experiments carried out by Allen et al. (2002) did not show any differences in measured COD, DOC or SO_4^- concentrations correlated to

depth. This indicates a complete mixing of pollutants through diffusion and dispersion within all columns, at least in the top 30 cm where the measuring pipes were installed. Homogeneity of concentrations should not be considered as a general rule for column modelling due to differences in root distribution of planted columns shown on pictures (see Annex I: Root distribution at the end of the physical experiments) and measured differences of electronegativity by depth (Allen et al., 2002). The deepest sampling point was at 20 cm to the bottom of the physical column where water was replenished which might mean only measured concentrations showed homogeneity. A diluted zone could have established closer to the injection point.

Evapotranspiration losses were linearly interpolated for all planted columns using approximated values described in Allen et al., (2002) for 4°C and 24°C. For unplanted columns correlations were adopted from Kadlec and Wallace (2009: 110) to estimate evaporation losses of unplanted gravel media. At first, A-Type evaporation pan losses (EA_A) were estimated using equations given in the book averaged for *Typha* and *Schoenoplectus*. Assuming no difference in evapotranspiration (ET) of planted columns (Allen et al, 2002), evaporation loss from an A-Type pan, EA_A can be described via Equation 3. The result of this equation can be used to estimate evaporation losses from unplanted gravel (E_G) as the last step of this empirical approach, shown by Equation 4 (Kadlec and Wallace, 2009: 110).

$$E_G = 0.0757 EA_A - 0.028\, mm\, day^{-1} \quad (3)$$

This is a rough estimation and the results were adopted only as guidance values for setting physical re-aeration in unplanted columns.

Root SNH uptake could have been adjusted relatively free because nitrogen removal was modelled as the simultaneous effect of root nitrogen uptake and oxygen supply. Practically there is no data available to share the contribution of the two processes to NH4-N removal. See Chapter 4.1 for exact values.

3.2.6 Iterative adjustment of model parameters and initial conditions

3.2.6.1 Iterative adjustment of model parameters and initial conditions

The process of adjusting model parameters included more than three hundred documented simulations until a parameter set was developed which enabled a fit between the simulated and measured data of all three planted columns, as well as the unplanted control column. Simulation records are available as MS Excel© worksheets on the DVD supplement in standardized format for scrutinizing, including all parameters, results and diagrams for evaluation. Only the important steps will be highlighted in time order as many of the changes to parameters had proven unsatisfactory or useless during these trials.

3.2.6.2 Setup of adsorption

Setting adsorption parameters preceded setting bacteria dynamics and fine-tuning initial concentrations as the process can be responsible for significant changes in a short period after start-up, leading to a plunge of some concentration values. Assigning priority

to the calibration of other parameters could have caused a setup with higher initial bacteria concentration with lysis-dominated dynamics, more intensive re-aeration or even changed biokinetic parameters to simulate a fast concentration decline. It is notable that adsorption isotherm parameters are hard to estimate without having any knowledge of bacteria dynamics – changes might be caused by simultaneous processes of adsorption, hydrolysis and other bacterial degradation – so a fine-tune of adsorption parameters was done again after biokinetic parameters were defined.

Adsorption was set for two contaminant species, COD and NH_4-N. In practice it is often assumed COD is absorbed into the biofilm and there further processed (Mburu et al., 2012), which was modelled setting up adsorption of XS. The linear isotherm defined by Mburu et al. (2012.) was satisfactory for all simulations; its parameters are included in Annex III: Model parameters. The initial concentration of adsorbed COD was set to be zero before each run.

Mburu et al. (2012) modelled ammonium nitrogen sorption using a Freundlich isotherm but with a reference on the work of McBride and Tanner (2000) who described it as a process involving three mediums – the water, the biofilm and the gravel surface. As the equation given by Mburu et al. (2012) is ignoring biofilm sorption and has a different form to the input of HYDRUS, a Langmuir correlation was parameterized and used for further work. A Microsoft Excel© sheet was used for monitoring and adjusting equilibrium concentrations at different adsorption parameters. It allowed entering many set of the parameters defining a Langmuir isotherm and to do adjustments on a trial-and-error basis.

The measured values showed a variation in the initial NH_4-N dynamics which was modelled by making adjustments to initial adsorbed ammonium nitrogen concentrations. These were similar for the different planted and the unplanted groups at all temperatures which was expected as all physical experiments followed the same cyclic routines and the solved concentrations were about the same at the end of each plant group. Initial condition settings including sorbed concentrations of ammonium nitrogen can be found in Chapter 4.2.

3.2.6.3 Initial bacterium concentrations

It is difficult to make any pre-assumptions of initial bacterium concentrations. A parameter estimating tool like the one AQUASIM has (Reichert, 1998) can facilitate model calibration (Mburu et al., 2012). Initial bacteria concentrations given in their work were taken for all columns as base values for first simulations and divided by ten because otherwise a significant die-off approximating to about the tenth of the starting value was modelled. The initial concentration of XASRB was about one lg lower as other bacteria leading to a slower decrease in sulphate concentration compared to measured values and for this reason its proportion was not divided by ten. The concentration was satisfactory in a few cases without additional changes.

Bacterial activity was an important factor for the changes in sulphate concentrations so $XASRB_{INI}$ regularly needed adjustment to fit the slope of the SSO4 curve to the measured values of the first days. This was complemented with the adjustment of initial XSOB concentrations in some instances like the one of well-aerated columns *Carex* 12°C

and 16°C, where it helped to simulate the more complex sulphate dynamics. Where $XSOB_{INI}$ and XH_{INI} had an instantaneous die-off their initial concentration was set lower without any unfavourable effect. Other initial bacteria concentrations were proven satisfactory in most cases and had only minor adjustments if any.

3.2.6.4 Biokinetic parameters

Biokinetic parameters were left as standard values (Langergraber and Šimůnek, 2011) for early simulations except some changes adopted from Mburu et al. (2012). The unplanted columns were selected to start working with due to their relative simplicity. The second group to model was columns planted with *Carex* because they had the most complex dynamics of measured sulphate concentrations at 12°C and 16°C which needed fine adjustment to reproduce – and the pre-assumption was if they are simulated properly the parameters will not need any further adjustments to simulate other planted columns. For the detailed calibration process see Chapter 4.1.

3.2.6.5 Column-specific adjustments

After adsorption and biokinetic parameters had been standardized only three parameters had to be fine-tuned for each column and temperature. These were initial bacterium concentrations, root oxygen release (cRoot for SO) and initial adsorbed SNH concentrations. For a detailed description see Chapter 4.1.

3.3 The evaluation of simulation results

3.3.1 Monitoring of setup adjustments

A standardized Microsoft Excel© workbook was created which made possible the rapid evaluation of each simulation run. This was necessary because of the high number of different outcomes from the partly trial-and-error approach and because the modelling tool handles COD as different fractions and does not give any graphical or summarized numerical results for it.

A new workbook was created after each major adjustment and for each species. Simulations were run until there was a good visual fit to physical measurements. Each workbook contains four types of worksheets:

1. A description sheet, including what was the overall goal of the simulations analysed using the workbook and the adjustments made for each run (if recorded);
2. An import sheet, which is linked to the complete parameter setup and simulation results and can be manually refreshed. The links point to files from the HYDRUS working directory listed and briefly explained (Šimunek et al., 2011), marking the rows of sheet type 2-4 where they are merged:
    a. ObsNod.out: contains observation node results (row 13-42)
    b. ATMOSPH.IN: atmospheric information input data (row 45-53)
    c. BOUNDARY.IN: boundary information input data (row 57-87)
    d. SELECTOR.IN: input data (row 91-278) of

i. Basic information
ii. Material information
iii. Time information
iv. Solute transport information
v. Heat transport information
vi. Root water uptake information

e. DIMENSIO.IN: dimension information input data (row 282-284)

3. Template sheets, containing
   a. marked spot where refreshed data can be inserted as non-linked data (values)
   b. a header and frame for this data
   c. a table of summarized COD, NH4-N and SO4-S concentrations
   d. a table with measured concentrations and their standard deviation for a selected column at given temperature
   e. diagrams showing the dynamics of bacteria types and contaminant groups mentioned above
4. A sheet formally identical to the template sheet, a record of a simulation setup and results including various goodness of fit analysis results.

The final worksheets contain the calculus and additional diagrams for goodness of fit analysis.

3.3.2 Statistical evaluation of final results

3.3.2.1 Used goodness of fit analyses

After a good fit was achieved between measured and simulated values the final results were evaluated not only visually but using numerical goodness of fit analyses. Ahnert et al. (2007) concluded in most publications only quotes about the quality of the fit are made or only Pearson's Correlation Coefficient (PCC) or the Coefficient of Determination (R^2, Forthofer et al., 2007) are used. This can result in subjective interpretation of model accuracy and therefore Ahnert et al. (2007) suggested a routine including five steps with different techniques. This routine cannot be completely overtaken for this work because of the characteristics of the experiments carried out:

- The batch operation results in most cases in a time-progressive change in concentrations meaning simple methods of descriptive statistics are useless for numerical analysis (e.g. the comparison of the mean or median of measured and simulated values). This coincides by differences in the time intervals between measurements as well.
- Multiple replicates of all column types had measurements parallel and the physical measurement data received (Mburu, 2013) has mean and standard deviation (SD) for each measurement. A suitable evaluation method should incorporate SD in the analysis, however, goodness of fit measures typically

ignore this (e.g. R^2, Root Mean Squared Error 'RMSE', Coefficient of Efficiency 'E').

To see the results of some of these typically applied numerical analyses two of them were chosen for use in this project, regardless of their expected weaknesses, as well as a new method was worked out which also considers SD. In total four methods were used to determine goodness of fit:

- Visual interpretation
- Coefficient of Determination (R^2),
- Coefficient of Efficiency (E) with both j=1 and j=2 (see Ahnert et al., 2007)
- Deflection analysis, a new method which considers SD of measured values, described in details in the next subchapter.

3.3.2.2 Coefficient of determination

The coefficient of determination can be calculated after taking simulated values as the function of measured values. A scatter plot can be created for easier interpretation where axis x is for measured data and y is simulated data. An inserted trendline represents the new model created by linear regression analysis and the coefficient of determination can be calculated based on it. This trendline gives the best possible fit to the data. However, the goodness of fit determined this way does not represent the goodness of fit of the simulation results to measured results, but the goodness of fit of an already imperfect model to the used model ignoring the level of imperfection. A perfect model could be described by $f(x) = x$ (all the measured data and simulated data is equal) – if the trendline has a different equation the analysis has an unknown error and R^2 describes only what part of the variance of *y* can be explained by the imperfect model which is the equation of the trendline. In such, if R^2 shows a good correlation the equation of the linear regression (trendline) can be scrutinized for how much it differs from $f(x) = 1x+0$ by comparing its slope to 1 and the constant to 0. If R^2 and the rise of the curve are close to one and the constant represents a low percentage of the measured values the method might still give a subjective result, as all three parameters have to be evaluated one after the other. Without giving the regression equation this method is completely unacceptable for model result evaluation as it gives a whitewashed goodness-of-fit except if $f(x) = 1x+0$ was used as the basis for comparison. Figure 6 shows an example when R^2 overrated the goodness of fit of a simulation which had overestimated measured values in general. Linear regression analysis whitewashes the error by shifting the trendline by +60.2 mg L^{-1}.

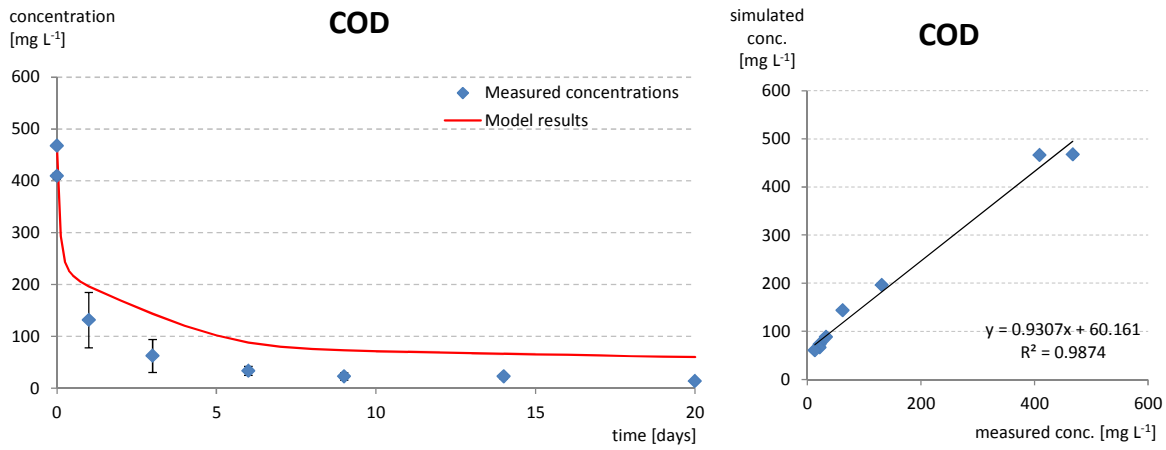

Figure 6: Case where the coefficient of determination (R^2) is overrating goodness of fit (*Carex* 16°C).

Coefficient of determination values ranged between 0.77 and 1.00 thus all of the regression equations could have been analysed. It is quite subjective which equation to consider as an indicator of weak results, thus only the four equations with the highest constants were selected. This is still not representative as different contaminants range on a different scale and the rise of the curve and R^2 is not considered. Any comparative analysis of different simulations is difficult and eventually this method was dropped. An objective formula could be created which compares the function of a perfect model, $f(x) = x$ to the function of the linear regression and takes R^2 into account but it exceeds the scope of this work.

3.3.2.3 Coefficient of efficiency

The coefficient of efficiency (E) is often used for hydraulic model result evaluation and can be considered as the coefficient of determination to the perfect model described by $f(x) = y$ if j=2. Its formulation is represented by Equation 4 (Ahnert et al., 2007).

$$E_j = 1 - \frac{\sum_{i=1}^{n} |M_i - E_i|^j}{\sum_{i=1}^{n} |M_i - \bar{M}|^j} \tag{4}$$

where M_i is the measured value, E_i is the simulated value. The numerator is identical to the residual sum of squares and the denominator to the total sum of squares because $M_i = y_i$ and j=2. The coefficient of efficiency is ranged between zero and one where one represents the perfect fit.

For the simulation results shown in Figure 6 the coefficient of efficiency $E_2 = 0.90$ and $E_1 = 0.66$. Ahnert et al. (2007) recommend to use E_1 but do not give a general rule which value should be considered as acceptable and which as a weak fit. The weakness of this method is it does not consider the SD of measurements.

Figure 7 serves as demonstration of a case where E underestimates goodness of fit. Visual interpretation shows that all simulated values were within the range of mean ± SD

and followed trends quite nice. However, calculated value of E_2 and E_1 is 0.74 and 0.54, respectively, indicating below average goodness of fit.

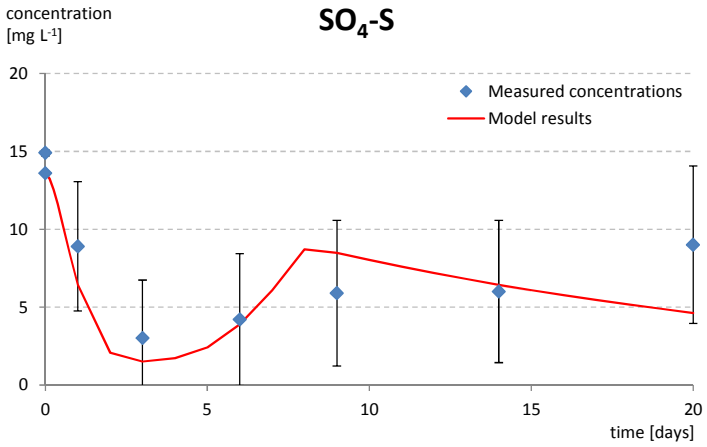

Figure 7: Case where the coefficient of efficiency (E) is underrating goodness of fit (*Carex* 12°C).

3.3.2.4 Deflection analysis

Deflection analysis is a goodness of fit-analysis for comparing simulation results to measured data of replicates or repeated experiments and was introduced for this thesis. It is suitable to evaluate simulation results based on mean and standard deviation values of repeated measurements.

The method is comparing the integral set by the curve of simulation results and the nearest one of the mean ± SD curves with the integral of (1) mean ± SD curves and (2) the curve set by average measured values over time using two parameters. The first comparison describes the proportion of the area sliced off by the deviation of simulation results from the region defined by the mean ± SD values and the area determined by the mean ± SD values. It can be interpreted both locally and for the whole data set. This parameter could be called *deflection*, and is expressed in %. Figure 8 denotes the two compared areas by pink (deviation) and grey (mean ± SD) on a fictional example:

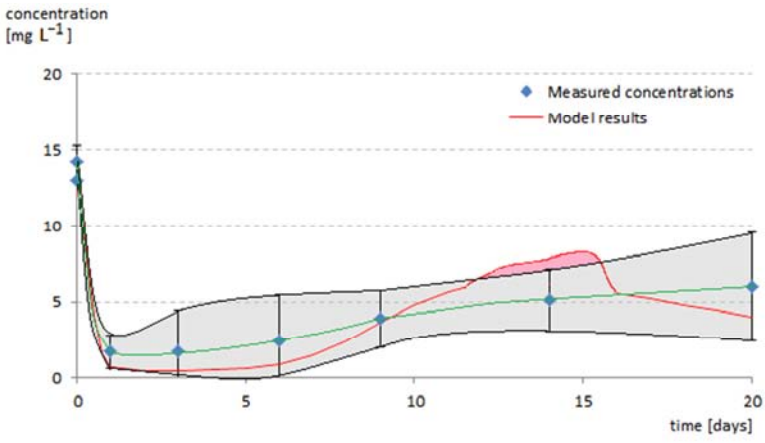

Figure 8: Visual explanation of *deflection*, the proportion of pink and grey areas.

The second comparison gives the proportion of the area set by deviation (pink) and the area below the curve set by mean values (green), both locally and for the whole

experiment. It could be called the ***magnitude of deflection*** and gives information about the significance of the previous parameter which is necessary in the case of a relatively small SD of measured values. Figure 9 shows the two compared areas by pink (deviation) and green (the area below mean values) on a fictional example.

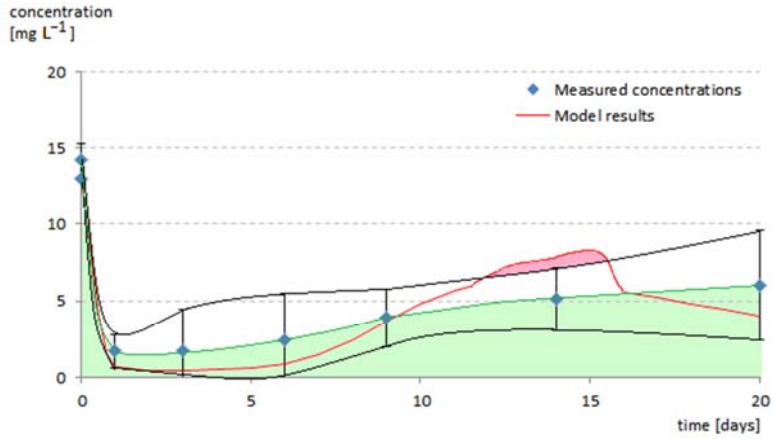

Figure 9: Visual explanation of the *magnitude of deflection*, the proportion of pink and green areas.

The time output of simulations must match the time of measured results to do the deflection analysis. As the number of modelled and measured values is finite (1) either interpolation should be applied for more precision or to get a missing value at a given time or (2) simply the measured and simulated values can be used without interpolations. The trapezoidal rule, described by Equation 5 is satisfactory for numerical integration and it forms the basis of deflection analysis.

$$\int_a^b f(x)dx \approx (b-a)\frac{f(a)+f(b)}{2} \tag{5}$$

Thus the area set by the deviation (marked by pink) is estimated using Equation 6 between two points and by Equation 7 for the whole data set.

$$DEV_{i,j} \approx (t_j - t_i)\left(\left|\frac{\bar{x_i} + SD_i + \bar{x}_j + SD_j}{4} - \frac{s_i + s_j}{4}\right| + \left|\frac{\bar{x_i} - SD_i + \bar{x}_j - SD_j}{4} - \frac{s_i + s_j}{4}\right|\right) - \frac{SD_{i,j}}{2} \tag{6}$$

$$DEV_{cum} \approx \sum_{i=1}^{n-1}(t_{i+1}-t_i)\left(\left|\frac{\overline{x_\iota}+SD_i+\bar{x}_{i+1}+SD_{i+1}}{4}-\frac{s_i+s_{i+1}}{4}\right| + \left|\frac{\overline{x_\iota}-SD_i+\bar{x}_{i+1}-SD_{i+1}}{4}-\frac{s_i+s_{i+1}}{4}\right|\right)-\frac{SD_{i,i+1}}{2} \quad (7)$$

The area enclosed by SD (marked by grey) is calculated locally using Equation 8 and for the whole data series using Equation 9.

$$SD_{i,j} \approx (t_j - t_i)(SD_i + SD_j) \quad (8)$$

$$SD_{cum} \approx \sum_{i=1}^{n-1}(t_{i+1}-t_i)(SD_i+SD_{i+1}) \quad (9)$$

The integral below measurement means can be estimated for neighbouring points by calculating the area of a local trapezoid (Equation 10) or the whole cumulative area below measured means (Equation 11) as follows:

$$MES_{i,j} \approx \left(t_j - t_i\right)\frac{\overline{x_\iota}+\bar{x}_j}{2} \quad (10)$$

$$MES_{cum} \approx \sum_{i=1}^{n-1}(t_{i+1}-t_i)\frac{\overline{x_\iota}+\bar{x}_{j+1}}{2} \quad (11)$$

Deflection represents the proportion of the area of deviation and SD and can be calculated for a complete simulation using Equation 12:

$$DEF = \frac{DEV_{cum}}{SD_{cum}} \quad (12)$$

The ***magnitude of deflection*** represents the proportion of deviation to the integral below means and can be calculated for a complete simulation using Equation 13:

$$MAG = \frac{DEV_{cum}}{MES_{cum}} \tag{13}$$

The highest acceptable values of DEV and MAG were chosen to be 50 and 25%. If these levels are exceeded the model is considered to fail. Values can range from 0% up more than 100%. Where SD or MES is 0 or unknown no local interpretation can be made.

Deflection analysis works fine with the examples shown on Figure 6 and Figure 7. Figure 10 shows the deflection (proportion of pink and grey areas) and the magnitude of deflection (proportion of pink and green areas). The goodness of fit of the underestimated COD removal efficiency is quantified by a DEF = 169% and MAG = 93%. Where coefficient of efficiency overestimated the goodness of fit (R^2=0.99) deflection analysis is in accordance with visual interpretation and indicates weak results as DEF is above 50% and MAG is above 25% at the same time.

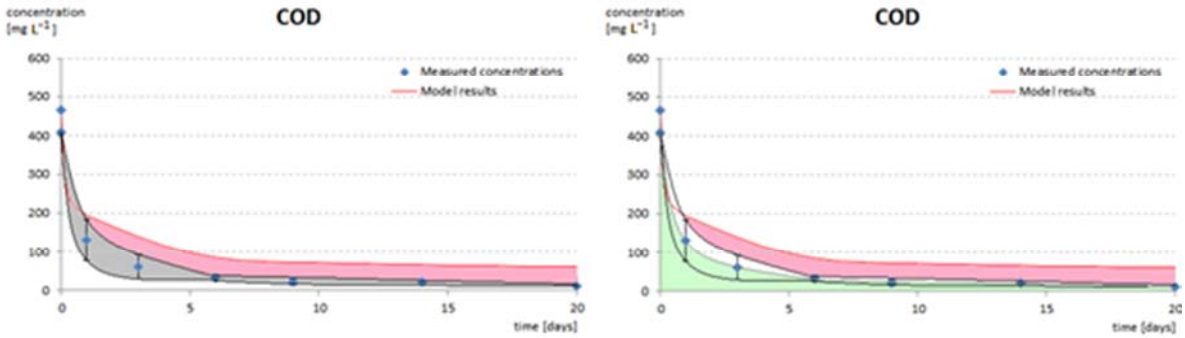

Figure 10: A deflection (DEF) of 169% (left) and a magnitude of deflection (MAG) of 93% (right) indicate together a weak goodness of fit.

Figure 11 shows the case with high SD values which made E_2 and E_1 to indicate a weak fit, however, as deflection analysis takes SD into account it gives DEF = 0% and MAG = 0% as result. This is in good accordance with visual interpretation because simulated concentrations never deviated from the grey area enclosed by measurement means ± SD.

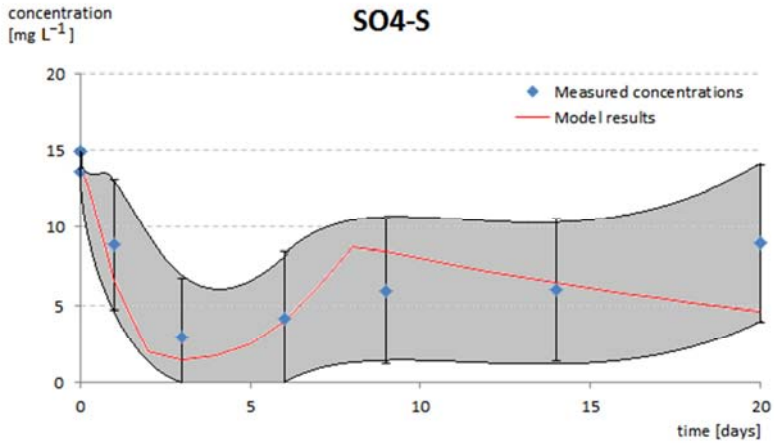

Figure 11: When simulation results stay within means ± SD, deflection analysis quantifies the goodness of fit as the best possible (DEF=0% and MAG=0%).

4 Results and Discussion

4.1 Calibration process

Biokinetic model parameters were left as standard values (Langergraber and Šimůnek, 2011) for early simulations except those for which changes had been made by Mburu et al. (2012). The unplanted columns were calibrated first because of their relative simplicity. The second group to continue calibration with was columns planted with *Carex* because they had the most complex dynamics of measured sulphate concentrations at 12°C and 16°C. It was expected that these will need the most effort to reproduce and once the simulation results fit the measured data well for the most complex time series no further adjustments of the parameters will be required to simulate other planted columns.

Simulation results of unplanted columns were in good agreement with measured data. The measurements of ammonium in unplanted columns made it probable that there were anaerobic conditions with no nitrification and complete sulphate reduction.

The calibration of the model was continued for columns planted with *Carex*. Compared to the unplanted columns the *Carex* columns had better oxygen supply as sulphate was not completely reduced and ammonium levels decreased significantly. The re-aeration rate calibrated insured the persistence of a small amount of oxygen during the whole batch with concantrations around 0.003-0.010 mg L^{-1}. This had significant implications on the outcomes by effecting bacterial activity using standard half-saturation and inhibition coefficients for anaerobic processes.

Simulated sulphate concentrations did not follow the dynamics of measured ones. The slope of XASRB was nearly constant with bacteria concentrations slightly decreasing with time. Sulphate concentrations were sharply decreasing even in relatively well-aerated columns like *Carex* 12°C on the first few days which meant some inhibition values had to describe the barrier as too low between aerobic and anaerobic environments. Moreover, measured sulphate concentrations reached zero contrary to the apparent convergence to a simulated low around 1.3 mg L^{-1} showed by simulations which can happen if a half-saturation coefficient is too high. Inhibition coefficients for SO and SNO and half-saturation coefficients for SSO4 were selected for calibration after examining their actual value and the reaction rate equation representing the growth of XASRB in Langergraber and Šimůnek (2011). Inhibition coefficients for SO (K_{OASRB}) and SNO (K_{NOASRB}) of XASRB had to be increased to trigger the simulated reproduction and metabolism of the bacteria group and the half-saturation coefficient for SSO4 (K_{SOASRB}) had to be decreased to allow a quicker sulphate reduction rate at low concentrations as well. Maximum growth rate of XASRB was increased to have a better match with initial measured sulphate concentration drop. No temperature dependence was calibrated for this parameter. The values of these parameters were adjusted a few times until all *Carex* column simulations fitted measured data well.

Parameters regulating nitrification had also to be changed to simulate the decrease in the concentration of ammonia in planted columns. Although the drop which generally happens within the first day was supported by setting up adsorption considering the effect of potential absorption into the biofilm, measured data of the *Carex* 20°C and 24°C columns showed a quick and steady further decrease in the following days. Simulated adsorbed SNH values showed that there is a significant contribution of nitrification and uptake by biomass growth to this initial decrease in all *Carex* columns. The data of *Carex* experiments at 24°C was used to calibrate the rate of SNH oxidation (nitrification) taking the slope of a curve touching the values of day one and day three. Early results showed that the nitrification rate had to be increased to fit these points. The responsible bacteria group is XA which was inhibited by low oxygen concentrations in the simulated domain. The problem was solved by significantly decreasing the half-saturation coefficient for SO (K_{OA}) and increasing maximum growth rate (μ_A).

For several biokinetic model parameters temperature dependency is calculated using the Arhenius equation (Šimunek et al., 2011). These were hydrolysis rate constant, maximum growth rates and lysis rates of bacteria for which the HYDRUS Wetland Module Manual (Langergraber and Šimůnek 2011) contains suggestions for both 10°C and 20°C. During the development of CWM1, no temperature dependencies were considered for XAMB, XASRB and XSOB as no literature data could be found (Langergraber, 2013).

Root SNH uptake was set up for all planted columns by applying the same cRoot value (4.693 mg L^{-1}) which represented an uptake within a range of 0.009-0.097 g m^{-2} day^{-1} or 5.5-14.2 mg in 20 days.

For modelling SNH adsorption a Langmuir correlation has been used. The Langmuir correlation has been shown to be more flexible than the Freundlich correlation as it allowed making changes to specific parts of the curve representing low concentrations (planted columns) and higher concentrations (unplanted columns) relative independently. The used parameters of the Langmuir isotherm are included in Annex III: Model parameters.

After adsorption and biokinetic parameters had been set, only three parameters had to be fine-tuned for each column and temperature. These were 1) initial bacterium concentrations, 2) root oxygen release (cRoot for SO) and 3) initial adsorbed SNH concentrations. The most affected bacteria groups were XASRB, XFB and XAB, mostly to fine-tune initial concentration changes, and XSOB, to match better the complex sulphate concentration changes in better aerated columns like *Carex* 12°C and 16°C. The values of cRoot for SO were set for the first simulations to match the re-aeration flux given by Mburu et al. (2012) but were significantly changed later. Due to the lower half-saturation coefficient of ammonium they had to be decreased in the better-aerated columns, including all planted at 12°C and *Carex* 16°C as well just as unplanted columns which root supply had to be decimated to have a constant ammonium-nitrogen concentration after the first few days. The oxygen flux was increased in other planted columns still representing a very low value. Initial sorbed ammonium nitrogen concentrations were set to have a good fit to the magnitude of the rapid change occurring within the first day in all columns. Initial

sorbed SNH and initial bacterium concentrations as well as root concentration parameter cRoot for SO are summarized in Table 9.

4.2 Model parameters

Table 6 shows biokinetic parameters at 20°C which were changed from standard values (Langergraber et al., 2009b; Langergraber and Šimůnek, 2011) either for this work or by Mburu et al. (2012) and used for the simulations.

Table 6: Biokinetic parameters used for the simulations compared to standard values given by Langergraber et al. (2009b) and used by Mburu et al. (2012).

Parameter name [unit]	Parameter tag	Standard (Langergraber et al. 2009b)	Mburu et al. (2012)	This work
Hydrolysis rate constant [day^{-1}]	K_h	3.00	0.58	0.58
Half-saturation coefficient of autotrophic bacteria for SO [mg L^{-1}]	K_{OA}	1.00		0.0026
Maximum growth rate for autotrophic bacteria [day^{-1}]	μ_A	1.00		1.50
Maximum growth rate for fermenting bacteria [day^{-1}]	μ_{FB}	3.00	3.77	3.77
Inhibition coefficient of acetotrophic methanogenic bacteria for SO [mg L^{-1}]	K_{OAMB}	0.0002		0.02
Inhibition coefficient of acetotrophic methanogenic bacteria for SNO [mg L-1]	K_{NOAMB}	0.0005		0.05
Maximum growth rate for acetotrophic sulphate reducing bacteria [day^{-1}]	μ_{ASRB}	0.18	0.31	0.50
Inhibition coefficient of acetotrophic sulphate reducing bacteria for SO [mg L^{-1}]	K_{OASRB}	0.0002		0.05
Inhibition coefficient of acetotrophic sulphate reducing bacteria for SNO [mg L^{-1}]	K_{NOASRB}	0.0005		0.50
Half-saturation coefficient of acetotrophic sulphate reducing bacteria for SSO4 [mg L^{-1}]	K_{SOASRB}	19.00		5.00
Yield coefficient for acetotrophic methanogenic bacteria	Y_{AMB}	0.032	0.04	0.04
Yield coefficient for acetotrophic sulphate reducing bacteria	Y_{ASRB}	0.05	0.04	0.04

The most significant were the changes in the half-saturation and inhibition coefficients for dissolved oxygen and nitrate (SO and SNO). These were increased or decreased by about two logs making possible nitrification and sulphate reduction at the same time. Root surfaces can act as a second type of environment in the filter media favouring for anoxic or aerobic processes. In the model there is no spatial segregation thus this was the way to include the effects of roots on microbial activity. These settings promoted microbial activity of XA because of much lower half-saturation concentration for SO and of XAMB and XASRB because of much higher inhibition concentrations for SO and SNO. Without these settings the activity of these bacteria would have been close to zero. The processes linked to these bacteria groups were necessary to follow the sulphate and ammonium-nitrogen dynamics of the real columns. Figure 12 shows the effect of a higher inhibition coefficient for SO (0.0002 → 0.05 mg L^{-1}) and SNO (0.0005 →

0.50 mg L^{-1}) and the lower half-saturation coefficient for the substrate SSO4 (19.0 → 5.0 mg L^{-1}) of acetotrophic sulphate reducing bacteria on the simulation results of *Carex* 24°C SO4-S.

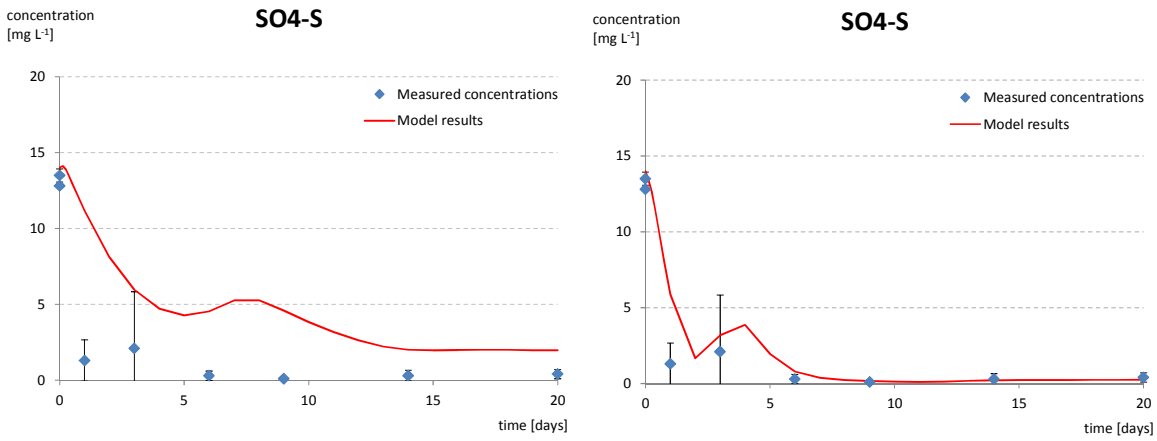

Figure 12: The combined effect of the final, higher inhibition coefficient for SO and SNO and the final, lower half-saturation coefficient for the substrate SO4-S of XASRB on the simulated SO4-S concentrations of *Carex* 24°C during calibration. Left: original, right: after applying the new parameters.

Table 7 shows the values used for root solute uptake concentration cRoot for SO, Table 8 the initial sorbed NH4-N concentrations and Table 9 the initial bacterium concentrations.

Table 7: Root solute uptake concentration for SO, cRoot [mg L^{-1}]

	12°C	16°C	20°C	24°C
Unplanted	-4.172	-27.600	-3.850	-3.800
Carex	-4.878	-4.380	-0.790	-0.879
Schoenoplectus	-5.118	-3.040	-0.733	-0.784
Typha	-5.632	-3.400	-1.182	-0.789

Table 8: Initial sorbed NH4-N concentrations [µg g^{-1}].

	12°C	16°C	20°C	24°C
Unplanted	32.70	38.50	40.00	38.50
Carex	1.00	1.50	1.80	2.00
Schoenoplectus	2.40	3.46	6.00	4.23
Typha	2.80	3.00	5.00	5.00

Table 9: Initial bacterium concentrations [μg g^{-1}]**.**

Heterotrophic bacteria XH_{INI}				
	12°C	16°C	20°C	24°C
Unplanted	5.48	0.20	1.26	5.48
Carex	4.47	5.00	0.68	0.68
Schoenoplectus	4.49	2.08	0.73	1.03
Typha	2.24	0.12	1.30	0.69
Autotrophic bacteria XAB_{INI}				
	12°C	16°C	20°C	24°C
Unplanted	1.01	1.20	0.57	1.01
Carex	0.40	0.60	0.58	0.53
Schoenoplectus	0.81	1.20	0.58	0.15
Typha	0.80	1.20	0.63	1.16
Fermenting bacteria XFB_{INI}				
	12°C	16°C	20°C	24°C
Unplanted	0.02	0.84	0.56	0.76
Carex	0.69	1.70	1.92	0.76
Schoenoplectus	1.53	0.84	0.84	0.84
Typha	0.08	0.84	0.66	0.76
Acetotrophic methanogenic bacteria $XAMB_{INI}$				
	12°C	16°C	20°C	24°C
Unplanted	0.89	0.88	1.08	1.44
Carex	3.05	2.80	2.04	1.44
Schoenoplectus	2.52	1.98	1.42	1.66
Typha	0.77	1.40	1.55	0.93
Acetotrophic sulphate reducing bacteria $XASRB_{INI}$				
	12°C	16°C	20°C	24°C
Unplanted	0.90	1.01	1.06	2.17
Carex	0.46	1.01	1.36	1.00
Schoenoplectus	0.99	0.80	1.01	1.01
Typha	0.84	1.12	1.01	0.77
Sulphide oxidizing bacteria $XSOB_{INI}$				
	12°C	16°C	20°C	24°C
Unplanted	0.04	0.03	0.04	0.04
Carex	0.37	0.10	0.07	0.10
Schoenoplectus	0.15	0.12	0.25	0.16
Typha	0.12	0.07	0.04	0.04

All parameters and initial conditions of all column setup are summarized in Annex III: Model parameters. Other parameters include settings of iteration, soil hydraulics, solute transport and reaction parameters, biokinetic model parameters, root solute uptake, boundary conditions, finite element mesh and all initial conditions.

4.3 Simulation results

In this chapter the main results from the master thesis are presented. Simulation results of all columns are marked by red continuous lines on Figure 13-Figure 15, for COD, NH4-N and SO4-S, respectively and in order of discussion. The means of measurements from the eight replicates of each column types are marked by blue with standard deviation displayed. A short visual evaluation of goodness of fit is also described for each figure.

4.3.1 COD concentrations

Results of simulated COD concentrations are collected in Figure 13. Most of the simulated data fits well to the measured data; however deviations occur in the case of several columns. These can be categorized in two groups:

1. Simulated concentrations do not follow the dynamics between day one and six which can be described as a slight increase or slowdown in the decrease of concentrations. Columns where this problem manifests most pronounced are Unplanted 12°C and *Typha* 12°C.
2. Simulated concentrations underestimate COD removal from day nine or through the whole batch, seemingly caused by an underestimated initial slump in the concentrations before day one. Columns where this problem is most notable are *Carex* 16°C, 20°C and 24°C.

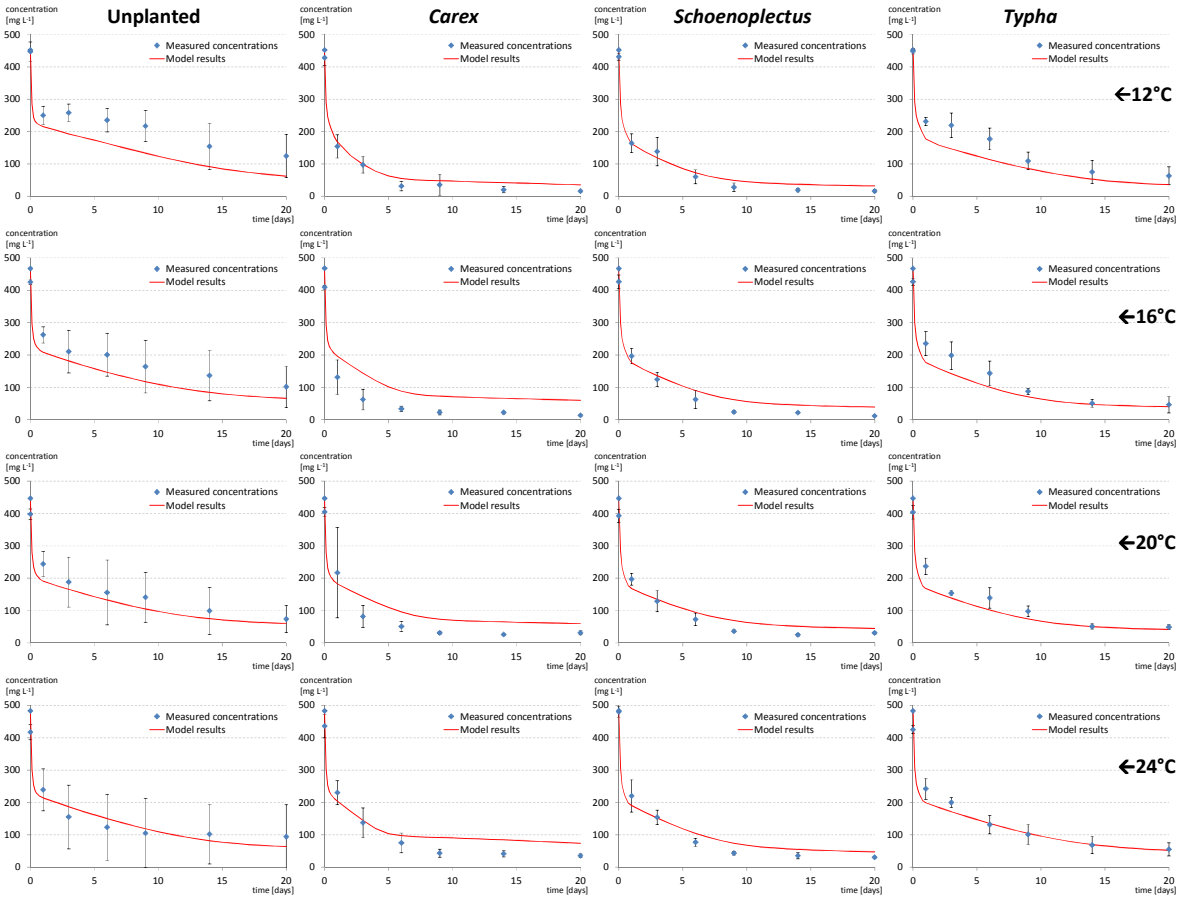

Figure 13: Simulation results for COD using CWM1 in HYDRUS.

4.3.2 NH4-N concentrations

Results of simulated NH4-N concentrations are collected in Figure 14. Model results fit very well to the measured data. The relative simple dynamics of ammonium nitrogen concentrations could be reproduced well by changing initial adsorped NH4-N

concentrations to scale the initial slump or rise. Later changes could be simulated by very slow nitrification and root nutrient uptake.

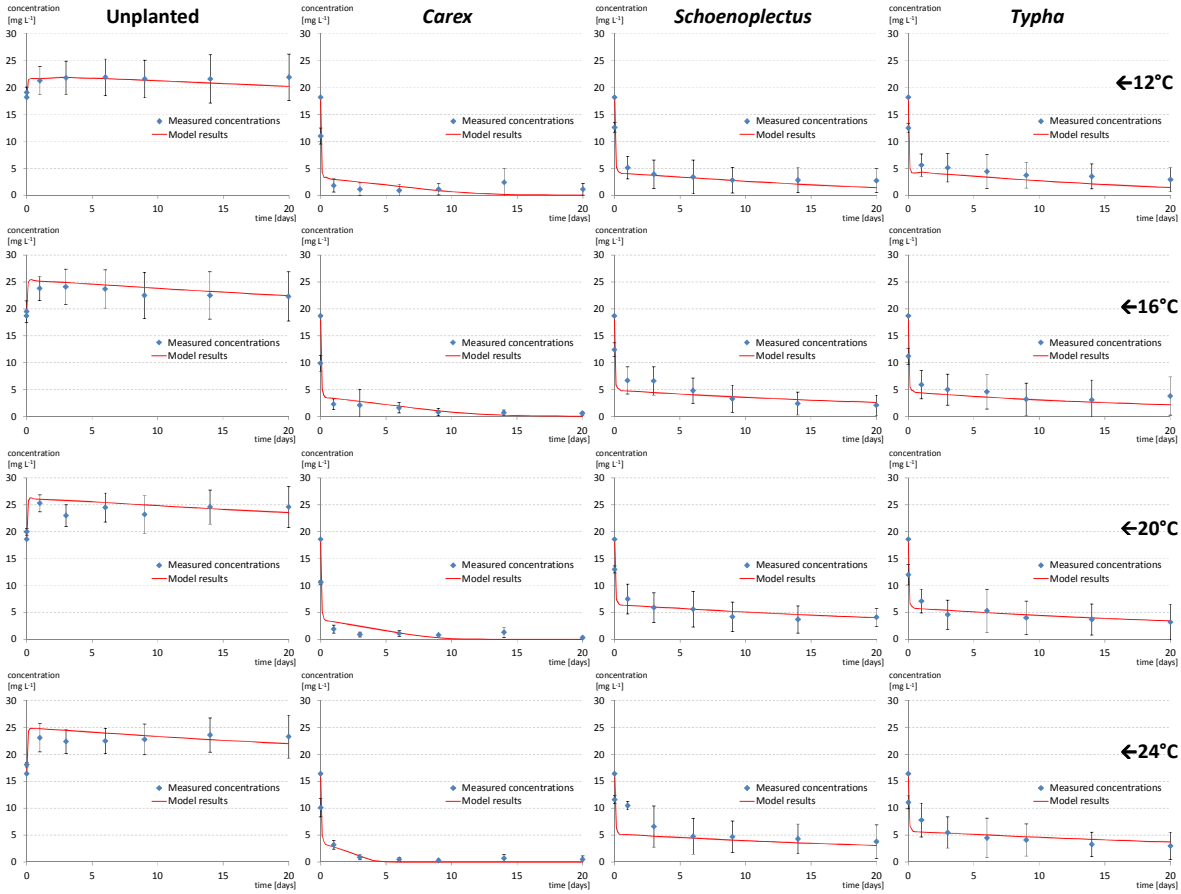

Figure 14: Simulation results of NH4-N using CWM1 in HYDRUS.

4.3.3 SO4-S concentrations

Results of simulated SO4-S concentrations are collected in Figure 15. All simulation results describe well sulphate dynamics in anaerobic columns with a quick transformation into hydrogen sulphide. Columns with better root re-aeration include *Schoenoplectus* 12°C and *Carex* 12°C and 16°C. The latter two had a complex dynamics which was simulated well until about day thirteen. After this point values still stay in the range set by SD but it is questionable if the processes are described properly because the slope of the simulated curve is negative but the means of the measurements are increasing. In the model available SNH is depleted and this results in bacterial inactivity and die-off of sulphide oxidizers, whilst in reality adsorped nitrogen might be directly available in the biofilm.

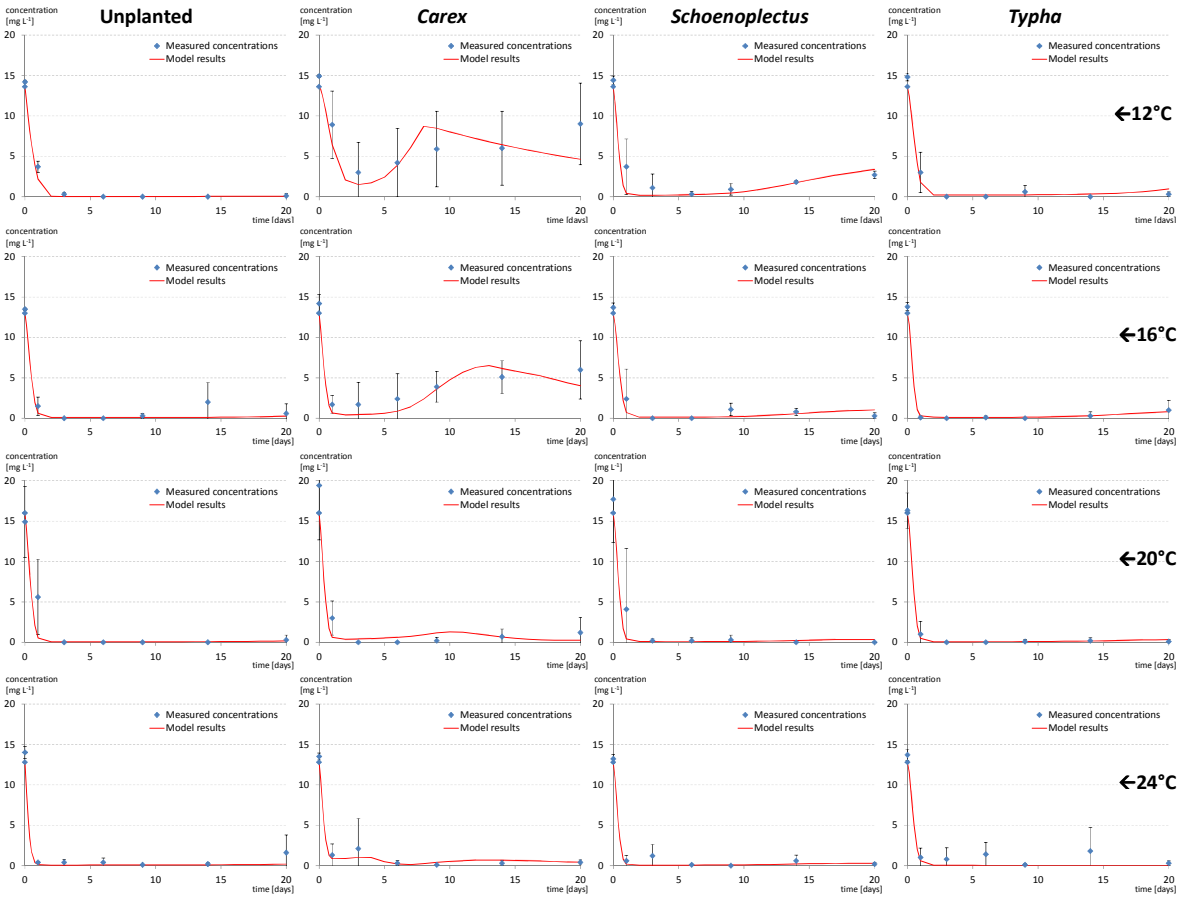

Figure 15: Simulation results of SO4-S using CWM1 in HYDRUS.

4.4 Goodness of fit

4.4.1 Overall goodness of fit

Visual goodness of fit evaluation shows a very good representativeness of the simulation results of the CWM1 implementation in HYDRUS in general. This is in accordance with the average of the results of the different numerical analyses carried out. Table 10 summarizes these results by contaminant species and includes values for an overall fit (column "Total"). Average values were not calculated for the coefficient of determination (R^2) as the equations of the linear regression on which it is based are different for all columns.

Table 10: Average goodness of fit by contaminant species for all columns.

All columns				
Goodness of fit parameter	**COD**	**NH4-N**	**SO4-S**	**Total**
E_2	0.94	0.76	0.96	0.89
E_1	0.77	0.61	0.86	0.75
DEF	35%	5%	5%	15%
MAG	17%	5%	5%	9%

Overall accuracy (Total) can be considered high. Coefficient of efficiency indicates the weakest fit was for NH_4-N whilst deflection analysis shows it was COD and changes in both NH_4-N and SO_4-S were simulated with a very high accuracy. The same statistic done only for planted columns shows better goodness of fit for COD, NH4-N and Total if using E and a worse fit using deflection analysis, shown in Table 11:

Table 11: Average goodness of fit by contaminant species for planted and unplanted columns

Unplanted columns				
Goodness of fit parameter	**COD**	**NH4-N**	**SO4-S**	**Total**
E_2	0.88	0.71	0.97	0.85
E_1	0.66	0.47	0.90	0.68
DEF	4%	0%	11%	5%
MAG	2%	0%	6%	3%
Planted columns				
Goodness of fit parameter	**COD**	**NH4-N**	**SO4-S**	**Total**
E_2	0.96	0.78	0.95	0.90
E_1	0.81	0.66	0.85	0.78
DEF	46%	7%	3%	18%
MAG	22%	7%	4%	11%

It is good to keep in mind for the interpretation of these data that E_2 and E_1 does not take the SD of measured values into account whilst DEF and MAG does. A table in Annex II: Results of goodness of fit analyses for each column is attached which contains results of all types of analyses for all columns.

4.4.2 Identifying and quantifying weak results

All goodness of fit analysis results were examined to select the weakest simulation results regarding contaminant type and to see if there is any difference between planted and unplanted columns. The table of Annex II: Results of goodness of fit analyses for each column contains results of all types of analyses for all columns and highlights the four weakest results by method and in the case of E_2 and E_1 the four weakest points by each column as well. All methods indicated different weak points but only one did it right and could be confirmed by visual evaluation.

Coefficient of efficiency indicated that the weakest results were achieved with the unplanted setups and the changes in NH_4-N concentrations were modelled poor in all columns. This is in discordance with the visual evaluation which shows that almost all simulated concentration values were within the range defined by SD and were close to the mean of the measurements at each time and had followed the dynamics of measured values of ammonium nitrogen. Unplanted columns were modelled especially with good accordance of results; the only exception was the COD at 12°C, which was not described

by E_2 and E_1 as the worst, but as described by Table 12. The results of deflection analysis are in accordance with visual interpretation.

Table 12: Coefficient of efficiency fails to quantify the visually poorest fit of unplanted column results, 12°C COD, while deflection analysis works fine.

Aspect	Method of analysis	Classification of unplanted 12°C COD
Poorest fit of unplanted columns	E_2	4th weakest
	E_1	3rd weakest
	Deflection analysis	weakest
Poorest fit of all columns	E_2	Not in the four weakest
	E_1	3rd* weakest
	Deflection analysis	Not in the four weakest

*: the four identified by E_1 as worst were all unplanted

Some COD concentrations were described as well-fitted by E although the removal was underestimated, e.g. COD for *Carex* 20 and 24°C and *Schoenoplectus* 16°C. The COD of *Carex* 16°C gave the weakest results of all contaminant species of all columns as simulated concentration values were about the double of measured ones after day three. Coefficient of efficiency and deflection analysis rated it as summarized in Table 13.

Table 13: Coefficient of efficiency fails to quantify the visually poorest fit of all results, *Carex* 16°C COD.

Aspect	Method of analysis	Classification of *Carex* 16°C COD
Poorest fit of *Carex* columns	E_2	Not in the four weakest
	E_1	3rd weakest
	Deflection analysis	weakest
Poorest fit of all columns	E_2	Not in the four weakest
	E_1	Not in the four weakest
	Deflection analysis	weakest

These results show how coefficient of efficiency failed to identify the weakest results and to match visual evaluation and that deflection analysis stood the test.

Whilst coefficient of determination with regression analysis and coefficient of efficiency failed to determine the weak point of the model, the deflection analysis identified the columns and contaminant species producing the worst results. A result where DEF was larger than 50% and MAG was larger than 25% was considered to be inaccurate and to have a significant difference between measured and simulated concentrations. This condition is fulfilled in the case of COD concentrations in *Carex* 16°C, 20°C and 24°C and *Schoenoplectus* 16°C columns.

There are some columns in which deflection analysis indicates that the goodness of fit is acceptable but rather weak. In the 20°C *Carex* column NH4-N is also close to the allowed limit of 50% DEF (49%) and MAG is already exceeding 25% (40%). These values are high because of the low concentration and SD values and the goodness of fit could be increased by decreasing initial adsorbed NH4-N concentrations. In the 20°C

Schoenoplectus column DEF is 62% but the 20% MAG stays below the accepted range. Visual interpretation shows a good fit and the high value of DEF can be attributed to low SD values.

4.4.3 Simulated COD removal

The removal efficiency of the columns was underestimated in a few cases, including 16, 20 and 24°C *Carex* and 16°C *Schoenoplectus* columns. In the case of all *Carex* columns SA and SF are both almost completely decomposed (SA_{av}=2.9 mg L^{-1}, SF<0.1 mg L^{-1}) which means most of the residual COD is in the form of non-adsorbed XS (XS_{av}=48.82). Scrutinizing the reasons it can be concluded that COD removal efficiency at day 20 is inversely related to temperature in the case of planted columns. The removal rate of the rapid decrease of concentrations occurring on the first few days seems to determine if the overall removal efficiency is simulated properly or not and concentration changes later on seem to have less significance. A reason for this can be adsorption or hydrolysis – as little is known about the adsorption capacity of the re-filled columns, hydrolysis was analysed further. Simulated hydrolysis rates of all columns were compared through time as shown by Figure 16:

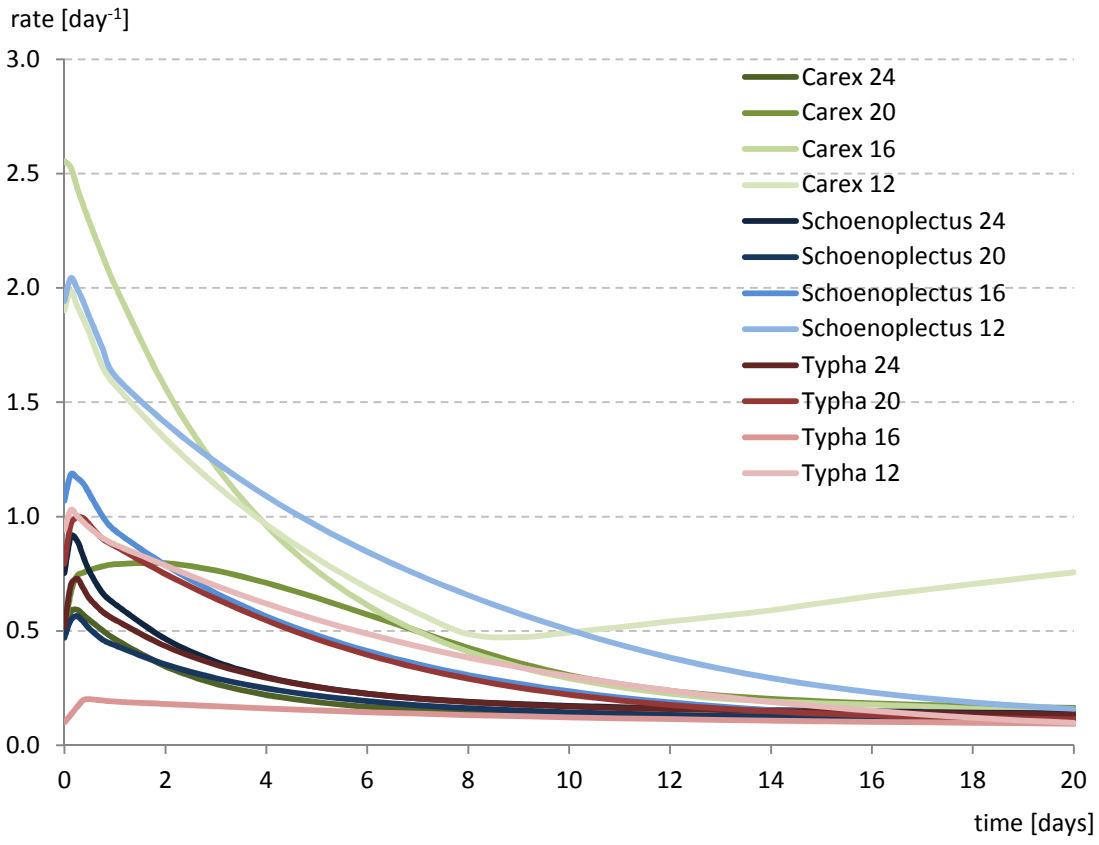

Figure 16: Simulated hydrolysis rates of all columns versus time.

The 16°C column planted with *Carex* shows a high rate of hydrolysis (starting at 2.5 day^{-1}). It still had a higher simulated residue of COD at the end of the batch (60 mg L^{-1}) as columns with much lower residual COD (e.g. *Schoenoplectus* 16°C with 39 mg L^{-1}, initial hydrolysis rate at about one). This means there is another reason behind the low

simulated COD removal efficiency of the four columns giving the worst fit, possibly driven by adsorption. The error could have been patched by increasing adsorption capacity and setting up initial adsorbed slowly biodegradable COD for all columns but this might be misleading as for example *Schoenoplectus* 12°C has a low residual COD concentration with current settings.

4.5 Issues of model setup and suggestions for improvement

The setup of simulated domains needed a think-through of the physical setup as well, which helped to identify some points which might have had an effect on the outcomes of physical and/or numerical model results. These are enumerated here with suggestions for improvement because the similarity of the physical setup and its numerical counterpart is important for model verification.

Columns represent a scale where the growing space of aboveground biomass is too large, whereas for underground organs it might be too tight, compared to full-scale systems. The humidity can also be different to the microclimate formed by large-scale stands and radiation was only about 25% of locally measured (Allen et al., 2002). This can change plant physiology and as an implication root nutrient uptake and oxygen and exudate supply. There is little what can be done against these effects. Planted columns could be arranged as close to each other as possible and surrounded by a foil as high as the plants are to mimic microclimatic humidity.

The reliability of calibrated root oxygen supply is impoverished because the water used in the physical experiments for evapotranspiration loss replenishment was not de-oxygenated. Table 14 shows the potential oxygen input through this pathway and compares it to the simulated cumulated flux supplied by roots in the case of the 24°C *Carex* model setup. De-oxygenated water should be preferred or the DO concentration sampled from time to time.

Table 14: Potential oxygen input through water replenishment with non-deoxygenated water.

Assumed DO concentration in replenishing water [mg L^{-1}]	Cumulative DO flux during batch [mg]	Cumulative DO flux expressed in % of the simulated root oxygen release
0.1	1.4	3 %
0.5	7.0	15 %
1.0	14.0	29 %
2.0	28.0	59 %
3.4	47.6	100 %

Evapotranspiration losses were not measured by plant species which means oxygen entering the microcosms via water replenishment could have had different effect on columns with different plants. If not de-oxygenated water is used for refilling, it is important to know potential oxygen intake via water replenishment. This can be calculated from the exact evapotranspiration losses and the oxygen content of the used water.

There is a large uncertainty about the three parameters: 1) initial adsorbed ammonium nitrogen concentrations, 2) initial bacterium concentrations and 3) root re-aeration, which were changed for each domain setup. It would be of high value for both constructed wetland research and modelling if these parameters could be measured. Furthermore, some of the conventional input parameters of the filter material, like bulk density and permeability are simply measurable and would be useful data for modelling.

5 Conclusions

Experiments with batch-operated constructed wetland microcosms have been previously carried out with different plant species at known temperatures and synthetic wastewater (Allen et al. 2002). Mburu et al. (2012) simulated data from these experiments using an implementation of the Constructed Wetland Model 1 (CWM1, Langergraber et al., 2009b) in the AQUASIM software (Reichert, 1998). This master thesis has verified the implementation of CWM1 in the HYDRUS wetland module (Langergraber and Šimůnek, 2012) using the same experimental data as Mburu et al. (2012).

Goodness of fit analyses showed that the HYDRUS implementation of CWM1 is working fine and provides an overall good fit that follows the contaminant dynamics of the measured concentrations in the batch-operated columns. The weak point was the simulation of the changes in COD, however this is not general in all columns but occurring rather in *Carex* 16°C, 20°C and 24°C and *Schoenoplectus* 20°C microcosms. COD is a component with many fractions (slowly biodegradable, readily biodegradable etc.) and involving all bacteria groups which makes this a complex issue. Simulated hydrolysis rate was not the driving force behind. This was not investigated in detail because it could have been solved by including initial adsorbed concentrations of XS.

These results show that parameters of CWM1 can be calibrated manually by starting with extremities using a trial-and-error approach. First the simplest column, the anaerobic unplanted was parameterized, then the one with the most complex SO_4 dynamics, *Carex* 12°C. After further minor adjustments to unplanted columns and to all *Carex* columns no changes were made to fit any of the *Schoenoplectus* or *Typha* columns. This means the final parameter set worked well in describing various anaerobic and anoxic columns with different plant species and different temperatures.

After creating a parameter set the goal was to adjust as few parameters as possible between the simulations of each column to achieve the desired goodness of fit. In contrast to Mburu et al. (2012) no adsorption parameters for SNH or slowly biodegradable COD had to be adjusted for different columns. It was satisfactory to adjust only initial SNH and bacterium concentrations in the solid phase and root oxygen loss parameter.

The final parameter set loosens DO concentration limits including half-saturation and inhibition coefficients for some bacterial processes. This was necessary to fit simulation results to measured values from planted columns. Some of the half-saturation and inhibition coefficients were adjusted in a way to let aerobic and anaerobic processes happen parallel. This can be justified considering root re-aeration and aerobic conditions at root surfaces.

Coefficient of determination (R^2, Forthofer et al., 2007) and coefficient of efficiency (E, Ahnert et al., 2007) were unable to evaluate the goodness of fit. Coefficient of determination gives a subjective result even if taking the regression equation into

account and as with the coefficient of efficiency it does not consider SD values. The deflection analysis method introduced for this work used the SD of measured data, and was able to describe goodness of fit and to identify the weakest simulation results.

Model results for root oxygen release cannot be considered as reliable due to some aspects of the physical experiment. The oxygen content of the water used for the compensation of evapotranspiration losses was unknown as well as the exact evapotranspiration rates by column type and temperature. Simulated root oxygen release includes also the oxygen intake by water used for the compensation of evapotranspiration losses. The use of distilled or de-oxygenated water is recommended for water replenishment in physical column experiments.

6 Outlook

Numerical models of constructed wetlands, including tools for biokinetic modelling are very complex, just as physical processes and environmental effects on these systems are also highly complex. In order to have a general model which can describe all types of systems a few developments are underway or under consideration, such as including preferential flow or deposition and biofilm processes.

In microbial ecology the term biokinetics means defining the rate of cell growth, substrate consumption and production (Abad et al., 2003). There is little information about the role of fungi in hydrolysis and their potential in the decomposition of inert organics which might be important. Furthermore, Toscano et al. (2009) cautions that simulation results are overestimating real treatment efficiency in the case of low-strength wastewater. These are two research topics which could add to the practical applicability of the model.

The modelling of biokinetics is based on the assumed presence and composition of bacterial communities and solving this issue by quantifying the concentration and activity of these bacteria by physical measurements can be the next step towards improved model accuracy and deeper understanding of constructed wetland processes in general. A precision experiment with macrocosms instead of columns could be carried out in which full material balances including weight of the pilot wetland, bacterium concentrations, gas exchange, adsorbed materials, adsorption equilibrium curves and various pollutants could be measured, such that it is synchronized with modelling and industrial demands.

The HYDRUS wetland module with CWM1 is a powerful tool, however practical design needs design guidelines or simplified models. Using these numerical tools will probably help to improve or create guidelines where it is necessary or to develop simplified models which can be used by engineers in the design process.

Acknowledgements

Many thanks to Zoltán Gribovszki at the University of West Hungary who first introduced me constructed wetlands, to Günter Langergraber at BOKU who guided me into the field of constructed wetlands and modelling, to Graeme Buchan at LU who was open-minded and hearted towards constructed wetlands, science and people in general and to Sam Carrick at Landcare Research for putting trust in me and taking me as his student from the other end of the globe.

Many thanks to my relatives, friends and people I have met in the recent years who made this individual master's more than a curricula: Biborka Kui, Zoltán Emődy-Wáman, Péter Csáfordi, Mom, Rehhát, Réka Sárffy, Maureen Vance, Stephan Lutter, the scholarship board at BOKU, my employers (only the nice ones), Roman Neunteufel, the colleagues at Sopron. It was the most amazing thing which could have happened to me in the last years, thank you.

References

Abad, A.; Cardona, S.C.; Domene, L.I.; López, F.; Navarro-Laboulais, J.; Torregrosa, J.I. (2003): Biokinetic parameters determination for wastewater characterisation. Analysis of COD and turbidity data. URL: http://personales.upv.es/jitorreg/Art%C3%ADculos/Biokinetic%20parameters%20determination%20for%20wastewater%20characterisation.PDF, Accessed: 26.05.2013

Ahnert, M.; Blumensaat, F.; Langergraber, G.; Alex, J.; Woerner, D.; Frehmann, T.; Halft, N.; Hobus, I.; Plattes, M.; Spering, V.; Winkler, S. (2007): Goodness-of-fit measures for numerical modelling in urban water management – a summary to support practical applications. Poster presented at the 10th IWA Specialised Conference on Design, Operation and Economics of large Wastewater Treatment Plants, Vienna, Austria, pp. 69-72. URL: http://www.hsgsim.org/downloads/Ahnert-etal_LWWTP07_paper.pdf, Accessed: 17.06.2013.

Albold, A.; Wendland, C.; Mihaylova, B.; Ergünsel, A.; Utrecht, H.G. (2011): Constructed wetlands: Sustainable wastewater treatment for rural and peri-urban communities in Bulgaria. WECF. URL: http://www.wecf.eu/download/2011/june/WECF_Constructed_Wetlands.engl..pdf, p. 9. Accessed: 27.05.2013

Allen, W.C.; Hook, P.B.; Biederman, J.A.; Stein, O.R. (2002): Temperature and wetland plant species effects on wastewater treatment and root zone oxidation. *J. Environ. Qual.* 31:1010-1016.

AquaCalc (2013) Conversions and Calculations – AquaCalc. URL: http://www.aqua-calc.com/page/density-table/substance/gravel-coma-and-blank-pea, accessed on: 27.01.2013

Brovelli, A.; Baechler, S.; Rossi, L.; Barry, D.A. (2009a): Comprehensive process-based modelling of sand filters and subsurface flow constructed wetlands. In: Bayona, J.M.; García, J. (ed.): *3rd International Symposium on Wetland Pollutant Dynamics and Control – WETPOL 2009. Book of abstracts* pp. 293-294, URL: http://infoscience.epfl.ch/record/162512/files/2009%20Brovelli%20etal%20WETPOL%20Procs%20Model.pdf, Accessed: 29.05.2013

Brovelli, A.; Malaguerra, F.; Barry, D.A. (2009b): Bioclogging in porous media: model development and sensitivity to initial conditions. *Environ Model Softw* 24(5):511-525.

Campbell, C.S.; Ogden, M. (1999): Constructed wetlands in the sustainable landscape. Wiley & Sons, New York, p. 45, 48-50, 54-55.

Chazarenc, F. (2013): *Personal communication.*

Forthofer, R.N.; Lee, E.S.; Hernandez, M. (2007): Biostatistics: A guide to design, analysis and discovery. 2nd edition. Elsevier, Sydney, NSW, Australia, pp. 349-386.

Grove, J.K.; Stein, O.R. (2005): Polar organic solvent removal in microcosm constructed wetlands. *Water Research* 39:4040-4050.

Henze, M.; Gujer, W.; Mino, T.; Loosdrecht, M. (ed.) (2000): *Activated sludge models ASM1, ASM2, ASM2d and ASM3*. IWA Publishing: London, UK.

Kadlec, R.H.; Wallace, S.D. (2009): *Treatment wetlands*. 2nd edition. CRC Press: Boca Raton, Florida, USA.

Langergraber, G. (2001): *Development of a simulation tool for subsurface flow constructed wetlands.* PhD thesis, Institute of Sanitary Engineering and Water Pollution Control, University of Natural Resources and Life Sciences: Vienna, Austria.

Langergraber, G. (2008): Modeling of processes in subsurface flow constructed wetlands – A review. *Vadose Zone J* 7(2), 830-842.

Langergraber, G. (2011): Numerical modelling: A tool for better constructed wetland design? *Water Sci Technol* 64(1), 14-21.

Langergraber, G. (2013): *Personal communication.*

Langergraber, G.; Šimůnek, J. (2005): Modeling variably-saturated water flow and multi-component reactive transport in constructed wetlands. *Vadose Zone J* 4(4):924-938

Langergraber, G.; Šimůnek, J. (2011): HYDRUS Wetland Module Manual, Version 2. *Hydrus Software Series 4*, Department of Environmental Sciences, University of California Riverside: Riverside, California, USA, 46 pp.

Langergraber, G.; Šimůnek, J. (2012): Reactive transport modelling of subsurface flow constructed wetlands using the HYDRUS wetland module. *Vadose Zone J* 11(2):special issue, 10.2136/vzj2011.0104

Langergraber, G.; Giraldi, D.; Mena, J.; Meyer, D.; Peña, M.; Toscano, A.; Brovelli, A.; Korkusuz, E.A. (2009a): Recent developments in numerical modelling of subsurface flow constructed wetlands. *Sci Tot Env* 407:3931-3943.

Langergraber, G.; Rousseau, D.; García, J.; Mena, J. (2009b): CWM1 – A general model to describe biokinetic processes in subsurface flow constructed wetlands. *Water Sci Technol* 59(9), 1687-1697.

Langergraber, G.; Pressl, A.; Haberl, R. (2011a): *Begleitende Untersuchungen zur praktischen Anwendung eines 2-stufigen bepflanzten Bodenfilters beim Gasthaus Bärenkogel. 1. Zwischenbericht.* Lebensministerium, Vienna, 26 pp. [in German]

Langergraber, G.; Pressl, A.; Leroch, K.; Rohrhofer, R.; Haberl, R. (2011b): Long-term behaviour of a two-stage CW system regarding nitrogen removal. *Water Sci Technol* 64(5): 1137-1141.

Llorens, E.; Saaltink, M.W.; García, J. (2011a): CWM1 implementation in RetrasoCodeBright: First results using horizontal subsurface flow constructed wetland data. *Chemical Engineering Journal* 166(1), 224-232.

Llorens, E.; Saaltink, M.W.; Poch, M.; García, J. (2011b): Bacterial transformation and biodegradation processes simulation in horizontal subsurface flow constructed wetlands using CWM1-RETRASO. *Bioresource Technol* 102(2), 928-936.

Mburu, N. (2013): *Personal communication.*

Mburu, N.; Sanchez-Ramos, D.; Rousseau, D.P.L.; van Bruggen, J.J.A.; Thumbi, G.; Stein, O.R.; Hook, P.B.; Lens, P.N.L. (2012): Simulation of carbon, nitrogen and sulphur conversion in a batch-operated experimental wetland mesocosm. *Ecol. Eng.* 42:304-315.

McBride, G.B.; Tanner, C.C. (2000): Modelling biofilm nitrogen transformations in constructed wetland mesocosms with fluctuating water levels. *Ecol. Eng.* 14: 93-160.

Meyer, D. (2011): *Modellierung und Simulation von Retentionsbodenfiltern zur weitergehenden Mischwasserbehandlung*. Dissertation, Technische Universität Kaiserslautern, Germany. [in German]

Meyer, D.; Sommer, T.; Thomas, M.; Schmitt, T.G.; Hagen, H. (2007): Development of a long-term pollution-load model to simulate CWs for CSO treatment. In: Mander, Ü.; Kóiv, M.; Vohla, C. (ed.): 2nd International Symposium On "Wetland pollutant dynamics and control WETPOL 2007" – extended abstracts, 16-20 September 2007, Tartu, Estonia, vol. I., p. 217-219.

ÖNORM B 2505 (2009): Bepflanzte Bodenfilter (Pflanzenkläranlagen) – Anwendung, Bemessung, Bau und Betrieb (Subsurface-flow constructed wetlands – Application, dimensioning, installation and operation. Austrian guidelines). Österreichisches Normungsinstitut Vienna, Austria [in German].

Pálfy, T.G.; Langergraber, G. (2013): Numerical simulation of the treatment performance of a horizontal flow constructed wetland for polishing SBR effluent. Extended abstract, accepted for oral presentation at the 5th International Symposium on Wetland Pollutant Dynamics and Control (WETPOL 2013), 13-17. October 2013, Nantes.

Polpraselt, C. (2006): Design and operation of constructed wetlands for wastewater treatment and reuses.; In: Ujang, Z.; Henze, M. (2006): Municipal wastewater management in developing countries. IWA Publishing, London, pp. 192-218.

Reed, S.C.; Crites, R.W.; Middlebrooks, E.J. (2006): *Natural Wastewater Treatment Systems.* CRC Press, Boca Raton, p. 367

Reichert, P. (1998): AQUASIM 2.0 – User manual. Swiss Federal Institute for Environmental Science and Technology (EAWAG). Dübendorf, Switzerland. ISBN: 3-906484-16-5.

Salvato, J.E.; Nemerow, N.L.; Agardy, F.J. (ed.) (2003): *Environmental Engineering*. Wiley and Sons: New Jersey, USA p. 269.

Šimůnek, J.; van Genuchten, M.Th.; Šejna, M. (2011): *The HYDRUS software package for simulating the two- and three-dimensional movement of water, heat, and multiple solutes in variably-saturated media.* Technical Manual, version 2.0. PC Progress: Prague, Czech Republic.

SSWM (2013): Sustainable Sanitation and Water Management Toolbox. URL: http://www.sswm.info/category/implementation-tools/wastewater-treatment/hardware/semi-centralised-wastewater-treatments/v, accessed on 26.07.2012

Stein, O.R. (2012): Identification of Microbial Functional Groups in Subsurface Flow Wetlands. Keynote presentation at the "Panamerican Conference on Wetland Systems for water quality improvement, management and treatment", 26 February - 1 March 2012, Pereira, Colombia.

Stein, O.R.; Borden-Stewart, D.J.; Hook, P.B.; Jones, W.L. (2007): Seasonal influence on sulfate reduction and zinc sequestration in subsurface treatment wetlands. *Water Research* 41:3440-3448.

Tanner, C.C.; Kloostermann, V.C. (1997): Guidelines for constructed wetlands for farm dairy wastewaters. NIWA Science and Technology Series 48, National Institute of Water and Atmospheric Research Ltd., New Zealand.

Tanner, C.C.; Headley, T.R.; Dakers, A. (2011): Guideline for the use of horizontal subsurface-flow constructed wetlands in on-site treatment of household wastewaters. Prepared for Gisborne District Council. http://www.niwa.co.nz/freshwater/update/freshwater-update-51-october-2011/constructed-wetlands-for-household-wastewater, accessed 02.08.2012

Tanner, C.C.; Sukias, J.P.S.; Yates, C.R. (2010): Constructed Wetland Treatment of Tile Drainage. NIWA Information Series 75, National Institute of Water and Atmospheric Research Ltd., New Zealand.

Tanner, C.C.; Sukias, J.P.S.; Headley, T.R.; Yates, C.R.; Scott, R. (2012): Constructed wetlands and denitrifying bioreactors for on-site and decentralized wastewater treatment: comparison of five alternative configurations. *Ecol. Eng.* 42:112-123.

Taylor, C.R.; Hook, P.B.; Stein, O.R.; Zabinski, C.A. (2011): Seasonal effects of 19 plant species in COD removal in subsurface treatment wetland microcosms. *Ecol. Eng.* 37:703-710.

Toscano, A.; Langergraber, G.; Consoli, S.; Cirelli, G.L. (2009): Modelling pollutant removal in a pilot-scale two-stage subsurface flow constructed wetland. *Ecol. Eng. 35:281-289.*

Annexes

Annex I: Root distribution at the end of the physical experiments

Photos courtesy of Otto R. Stein.

A

B

C

A: *Schoenoplectus acutus* (Muhl. ex Bigelow) A. & D. Löve *var acutus*

B: *Typha latifolia* L.

C: *Carex rostrata* Stokes

Annex II: Results of goodness of fit analyses for each columns

Coefficient of Determination

		Unplanted			Carex			Schoenoplectus			Typha		
		COD	NH4-N	SO4-S	COD	NH4-N	SO4-S	COD	NH4-N	SO4-S	COD	NH4-N	SO4-S
Regression equation	12°C	1.23x - 107.98	0.96x + 0.51	0.98x - 0.22	0.98x + 17.32	1.15x + 0.14	0.91x - 0.09	0.99x + 10.70	1.19x - 0.95	1.00x - 0.65	1.08x - 50.02	1.24x - 1.90	0.95x + 0.02
	16°C	1.20x - 76.30	1.28x - 5.55	1.01x - 0.48	0.93x + 60.16	1.15x + 0.57	1.03x - 0.90	0.97x + 23.71	1.12x - 0.50	0.98x - 0.24	1.07x - 33.01	1.21x - 1.23	0.96x + 0.06
	20°C	1.13x - 43.45	1.14x - 2.66	1.02x - 0.54	0.92x + 40.34	1.15x + 0.44	0.89x - 0.01	0.99x + 16.56	1.11x - 0.03	0.95x - 0.41	1.07x - 28.39	1.12x - 0.04	0.99x - 0.02
	24°C	1.07x - 7.88	1.17x - 3.31	0.98x - 0.37	0.95x + 32.15	1.17x - 0.21	0.97x - 0.09	0.95x + 18.78	1.09x - 1.33	1.00x - 0.28	1.06x - 12.6	1.07x + 0.24	1.02x - 0.75
R^2	12°C	0.99	0.83	0.99	1.00	0.89	0.80	0.99	0.93	0.96	0.98	0.92	0.99
	16°C	0.98	0.97	0.99	0.99	0.87	0.97	0.99	0.87	0.98	0.97	0.86	1.00
	20°C	0.98	0.80	0.93	0.97	0.89	0.97	0.98	0.90	0.97	0.97	0.88	1.00
	24°C	0.97	0.85	0.99	0.98	0.92	0.99	0.99	0.77	1.00	0.97	0.86	0.99

Coefficient of Efficiency

		Unplanted			Carex			Schoenoplectus			Typha		
		COD	NH4-N	SO4-S	COD	NH4-N	SO4-S	COD	NH4-N	SO4-S	COD	NH4-N	SO4-S
E_2	12°C	0.76	0.72	0.99	0.99	0.80	0.74	0.99	0.86	0.95	0.92	0.81	0.99
	16°C	0.89	0.77	0.98	0.90	0.74	0.94	0.98	0.79	0.98	0.94	0.71	1.00
	20°C	0.94	0.62	0.92	0.94	0.78	0.96	0.97	0.83	0.96	0.95	0.78	1.00
	24°C	0.95	0.72	0.98	0.96	0.84	0.99	0.99	0.61	0.99	0.97	0.78	0.97
E_1	12°C	0.48	0.54	0.94	0.90	0.65	0.54	0.90	0.75	0.84	0.72	0.62	0.90
	16°C	0.63	0.49	0.89	0.66	0.69	0.74	0.84	0.62	0.88	0.78	0.60	0.96
	20°C	0.75	0.40	0.85	0.75	0.68	0.83	0.83	0.73	0.87	0.80	0.68	0.97
	24°C	0.79	0.44	0.90	0.80	0.76	0.92	0.89	0.53	0.93	0.86	0.64	0.85

Deflection Analysis

		Unplanted			Carex			Schoenoplectus			Typha		
		COD	NH4-N	SO4-S	COD	NH4-N	SO4-S	COD	NH4-N	SO4-S	COD	NH4-N	SO4-S
DEF	12°C	16%	0%	37%	12%	4%	0%	19%	1%	0%	19%	1%	13%
MAG		8%	0%	14%	8%	8%	0%	10%	1%	0%	9%	1%	14%
DEF	16°C	0%	0%	1%	169%	11%	0%	75%	0%	2%	9%	1%	0%
MAG		0%	0%	2%	93%	15%	0%	27%	0%	2%	4%	1%	1%
DEF	20°C	0%	0%	5%	68%	49%	9%	62%	0%	5%	15%	0%	2%
MAG		0%	0%	7%	44%	40%	15%	20%	0%	10%	4%	1%	2%
DEF	24°C	0%	0%	2%	53%	9%	2%	45%	2%	0%	2%	0%	0%
MAG		0%	0%	3%	26%	10%	4%	14%	2%	0%	1%	0%	0%

Four weakest of all columns

Four weakest by plant species

Annex III: Model parameters

Iteration Criteria		
Iteration Criteria		
Maximum Number of Iterations		7
Water Content Tolerance	-	0.001
Pressure Head Tolerance	cm	1
Time Step Control		
Lower Optimal Iteration Range		3
Upper Optimal Iteration Range		7
Lower Time Step Multiplication Factor		1.3
Upper Time Step Multiplication Factor		0.7
Internal Interpolation Tables		
Lower Limit of the Tension Interval	cm	0.0001
Upper Limit of the Tension Interval	cm	10000
Initial Condition		In Pressure Heads
Soil Hydraulic Model		
Hydraulic Model		van Genuchten - Mualem, Without Air-Entry Value of -2 cm
Hysteresis		No Hystereis
Water Flow Parameters		
Material Properties for Water Flow		
Number of Materials		1
Name		Pea gravel
Residual Water, Qr	-	0.045
Porosity, Qs	-	0.27
Alpha	cm^{-1}	0.145
n	-	2.68
Saturated Hydraulic Conductivity, Ks	$cm\ d^{-1}$	172,800
l	-	0.5
Temperature Dependence		No Temperature Dependence
Solute Transport		
Time Weighting Scheme		Crank-Nicholson Scheme
Space Weighting Scheme		Galerkin Finite Elements
Solute Information		
Number of Solutes		17
Pulse Duration	day	1
Mass Units		µg
Stability Criterion		2
Use Tortuosity		Millington & Quirk
Wetland Module		CWM1
Iteration Criteria (for Nonlinear Adsorption only)		
Absolute Concentration Tolerance		0.001
Relative Concentration Tolerance		0.001
Maximum Number of Iterations		10
Initial Conditions		In Liquid Phase Concentrations [Mass_solute/Volume_water]

Solute Transport Parameters																
Soil Specific Parameters																
Bulk. D.	g cm^{-3}								1.79							
Disp. L.	cm								500							
Disp. T.	cm								400							
Solute Specific Parameters																
Diffusion of Oxygen in Water	cm^2 d^{-1}								1.7304							
Diffusion of Organics in Water	cm^2 d^{-1}								1.0944							
Diffusion of Nutrients in Water	cm^2 d^{-1}								1.9224							
Diffusion of Oxygen in Gasous Phase	cm^2 d^{-1}								18456							
Diffusion of Organics in Gasous Phase	cm^2 d^{-1}								0							
Diffusion of Nutrients in Gasous Phase	cm^2 d^{-1}								0							
Reaction Parameters for Solute - Dissolved Oxygen																
				12°C					16°C				20°C			24°C
		unplanted	*Carex*	*Typha*	*Schoenoplectus*	unplanted	*Carex*	*Typha*	*Schoenoplectus*	unplanted	*Carex*	*Typha*	*Schoenoplectus*	unplanted	*Carex*	*Typha*	*Schoenoplectus*
Boundary Conditions																
cRoot	µg cm^{-3}	-4.17	-4.88	-5.63	-5.12	-27.60	-4.38	-3.40	-3.04	-3.85	-0.79	-1.18	-0.73	-3.80	-0.88	-0.79	-0.78
Reaction Parameters for Solute - Ammonium and Ammonia Nitrogen (NH4)																
Boundary Conditions																
cRoot	µg cm^{-3}								4.693							
Reaction Parameters																
Kd	cm^3 μg^{-1}								0.9							
Nu	cm^3 μg^{-1}								0.003							
Beta	-								1.2							
Alpha	d^{-1}								2							
Reaction Parameters for Solure - Slowly Biodegradable Particulate COD																
Reaction Parameters																
Kd	cm^3 μg^{-1}								0.575							
Beta	-								1							
Alpha	d^{-1}								2.4							
Solute Transport - Constructed Wetland Model No1 (CWM1) Parameters I																
Hydrolysis																
Hydrolysis Rate Constant									0.58							
Sat./Inh. Coef. Hydrolysis									0.1							
XFB Correction Factor									0.1							
Heterotrophic Bacteria (aerobic growth and denitrification)																
Max. Aerobic Growth Rate									6							
Anoxic Correction Factor									0.8							
Rate Constant for Lysis									0.4							
Sat./Inh. Coef. for SO									0.2							
Sat./Inh. Coef. for SF									2							
Sat./Inh. Coef. for SA									4							
Sat./Inh. Coef. for SNO									0.5							
Sat./Inh. Coef. for SNH									0.05							
Sat./Inh. Coef. For SH2S									140							

Auotrophic Bacteria	
Max. Growth Rate XA	1.5
Rate Constant for Lysis	0.15
Sat./Inh. Coef. for SO	0.0026
Sat./Inh. Coef. for SNH	0.5
Sat./Inh. Coef. For SH2S	140
Fermenting Bacteria	
Max. Growth Rate XFB	3.77
Rate Constant for Lysis	0.02
Sat./Inh. Coef. for SO	0.2
Sat./Inh. Coef. for SF	28
Sat./Inh. Coef. for SNO	0.5
Sat./Inh. Coef. for SNH	0.01
Sat./Inh. Coef. for SH2S	140
Acetotrophic Methanogenic Bacteria	
Max. Growth Rate XAMB	0.085
Rate Constant for Lysis	0.008
Sat./Inh. Coef. for SO	0.02
Sat./Inh. Coef. for SA	56
Sat./Inh. Coef. for SNO	0.05
Sat./Inh. Coef. for SNH	0.01
Sat./Inh. Coef. for SH2S	140
Acetotrophic Sulfate Reducing Bacteria	
Max. Growth Rate XASRB	0.5
Rate Constant for Lysis	0.012
Sat./Inh. Coef. for SO	0.05
Sat./Inh. Coef. for SA	24
Sat./Inh. Coef. for SNO	0.5
Sat./Inh. Coef. for SNH4	0.01
Sat./Inh. Coef. for SSO4	5
Sat./Inh. Coef. for SH2S	140
Sulfide Oxidizing Bacteria	
Max. Aerobic Growth Rate	5.28
Anoxic Correction Factor	0.8
Rate Constant for Lysis	0.15
Sat./Inh. Coef. for SO	0.2
Sat./Inh. Coef. for SNO	0.5
Sat./Inh. Coef. for SNH	0.05
Sat./Inh. Coef. for SH2S	0.24
Solute Transport - Constructed Wetland Model No1 (CWM1) Parameters II	
Temperature Dependence	
Hydrolysis	28000
KX (Hydrolysis)	-54400
XH	47800
XA	75800
KNHA (nitrification)	-160000
KFB Growth	47800

XFB Lysis										0								
XAMB										0								
XASRB										0								
XSOB										0								
Stoichiometric Parameters																		
Production of SI (Hydrolysis)										0								
Fraction of SF Generated (Lysis)										0.05								
Fraction of SI Generated (Lysis)										0.1								
Yield Coefficients																		
Yield Coefficient for XH										0.63								
Yield Coefficient for XA										0.24								
Yield Coefficient for XFB										0.053								
Yield Coefficient for XAMB										0.04								
Yield Coefficient for XASRB										0.04								
Yield Coefficient for XSOB										0.12								
Composition Parameters																		
N Content of SF										0.03								
N Content of SI										0.01								
N Content of XS										0.079								
N Content of XI										0								
N Content of Biomass										0.07								
Oxygen																		
O2 Saturation	µg cm^{-3}									9.18								
Temp. Dep. O2 Saturation										-15000								
Rate O2										0								
Root Water and Solute Uptake Model																		
Water Uptake Reduction Model										S-Shaped								
Critical Stress Index										1								
Solute Stress Model										No Solute Stress								
Root Water Uptake Parameters																		
S-Shape Parameters																		
P50	cm									-800								
P3	-									3								
PW	cm									-1.00E+10								
Time Variable Boundary Conditions																		
		unplanted	*Carex*	12°C *Typha*	*Schoenoplectus*	unplanted	*Carex*	16°C *Typha*	*Schoenoplectus*	unplanted	*Carex*	20°C *Typha*	*Schoenoplectus*	unplanted	*Carex*	24°C *Typha*	*Schoenoplectus*	
Parameters																		
Time	d									20								
Precip.	cm d^{-1}									0								
Evap.	cm d^{-1}									0								
Transp.	cm d^{-1}			1.66				1.85				2.04				2.23		
hCritA	cm									-0.01								
Surface area associated with transpiration	cm^2									314								
all other parameters										0								

Rectangular Domain Discretization																
Horizontal Discretization in X																
Count								21 (at every 0.50 cm)								
Vertical Discretization in y																
Count								31 (at every 1.66 cm)								
Initial concentrations																
			12°C				16°C				20°C				24°C	
		unplanted	*Carex*	*Typha*	*Schoenoplectus*	unplanted	*Carex*	*Typha*	*Schoenoplectus*	unplanted	*Carex*	*Typha*	*Schoenoplectus*	unplanted	*Carex*	*Typha*	*Schoenoplectus*
SO	µg cm^{-3}								1							
SF				113.0				116.9				111.8				120.8	
SA				45.2				46.7				44.7				48.3	
SI				18.1				18.7				17.9				19.3	
SNH (in liquid phase)				18.2				18.7				18.6				16.4	
SNH (in solid phase)		32.7	1.0	2.8	2.4	38.5	1.5	3.0	3.5	40.0	1.8	5.0	6.0	38.5	2.0	5.0	4.2
SNO									0.0								
SSO4				13.6				13.0				16.0				12.8	
SH2S									0.0								
XS (in liquid phase)				275.7				285.1				272.7				294.6	
XS (in solid phase)									0.0								
XI									0.0								
XH		5.48	4.47	2.24	4.49	0.20	5.00	0.12	2.08	1.26	0.68	1.30	0.73	5.48	0.68	0.69	1.03
XA		1.10	0.40	0.80	0.81	1.20	0.60	1.20	1.20	0.57	0.58	0.63	0.58	1.01	0.63	0.16	0.15
XFB		0.02	0.69	0.08	1.53	0.84	1.70	0.84	0.84	0.56	1.92	0.66	0.84	0.76	0.76	0.76	0.84
XAMB		0.89	3.05	0.77	2.52	0.88	2.80	1.40	1.98	1.08	2.04	1.55	1.42	1.44	1.44	0.93	1.66
XASRB		0.90	0.46	0.84	0.99	1.01	1.01	1.12	0.80	1.06	1.36	1.01	1.01	2.17	1.00	0.77	0.77
XSOB		0.04	0.37	0.12	0.15	0.03	0.10	0.07	0.12	0.04	0.07	0.04	0.25	0.04	0.10	0.04	0.16

Annex IV: DVD

Contents of the DVD

Folders:

01 Archived Calibration Results: Standard format MS Excel © sheets for scrutinizing the outcomes of different calibration steps. Smaller index means earlier stage of the setup.

02 Final Domain Setups: HYDRUS-format h3d2 working directories for all sixteen columns.

03 Final Simulation Results: Standard format MS Excel © sheets with final results of all planted and unplanted columns, including bacterium concentration charts.

Files:

01 PALFY 2013 Verification of the Implementation of CWM1 in the HYDRUS Wetland Module.pdf: PDF version of this master's thesis.

02 Measured data_Simulation & Validation_MSU_Mburu 2013.xls: Detailed values of measured concentrations registered during the physical column experiments at MSU. Courtesy of Njenga Mburu.

Curriculum Vitae

Full Name:	Tamás Gábor Pálfy
Permanent Postal Address:	8230 Balatonfüred, Bajcsy-Zs. u. 20., Hungary
Tel:	+43 680 241 8467
E-Mail:	palfy.tamas@gmail.com
Nationality:	Hungarian

Education

International Master for Natural Resource Management and Ecological Engineering

Joint Master (in English)

02.07.2012-02.11.2012: Lincoln University, Christchurch, New Zealand

01.03.2011-15.09.2013 (exp.): University of Natural Resources and Life Sciences Vienna

- Focus of studies: design and modelling of constructed wetlands
  - Topic of thesis: Verification of the Implementation of Constructed Wetland Model One (CWM1) in the Hydrus Wetland Module
  - Special topic at Lincoln: Water, solute, colloid, and microbial transport in the critical zone: Design of and Processes in Constructed Wetlands. General overview of CWs with a focus on NZ relations and modelling a HF system in CWM1.
  - Project work at BOKU: Planning and Design in Water Supply and Wastewater Treatment. Design of a vertical flow system with mechanical pre-treatment for a village (725 PE).

Enrolled to Master's Programme Nature Conservation Engineering

01.02.2010-10.06.2011, University of West Hungary. Attended a topic "Extensive wastewater treatment". Left the program for the joint master's.

Bachelor of Science: Nature Conservation Engineering

04.09.2006-29.01.2010, University of West Hungary, with excellent grade

Thesis topic: wetland ecology and hydrology including one and a half year self-conducted research of marshes and fens at protected area.

Professional Experience

University of West Hungary, Institute of Geomatics and Civil Engineering

01.03.2013-15.09.2013 (exp.) Modelling and design of a horizontal flow constructed wetland for tertiary effluent treatment of a sequencing batch reactor. ERASMUS Placement.

Sustainable Europe Research Institute (SERI), Vienna, Austria

01.07.2011-29.02.2012 Research assistant: creating and evaluating diagrams and databases of environmental and material statistics, thematic research, writing reports and web content, designing slides. Language of created materials: English.

University of West Hungary, Institute of Botany and Nature Conservation, Sopron, Hungary

14.09.2009-23.10.2009 Internship: creating photo database; seedling monitoring

Balaton Uplands National Park Directorate, Csopak, Hungary

03.08.2009-14.09.2009 Internship: population estimating, habitat mapping, tour guiding.

Other Skills and Qualifications

Languages: Hungarian (native), English (excellent), German (fluent)

IT Proficiency

Modelling and drafting: Hydrus 2.xx Wetland Module, AutoCAD 2012 (2D)
GIS: ArcView 3.x, ArcGIS 10, Surfer 8.x (advanced)
MS Office: Excel incl. macro programming, Word, PowerPoint and Outlook (advanced)
Others: Visual Basic (basics), CorelDraw X4 (basics), Statictica (basics)

Driving license: B (European)

Mushroom expert (vocational qualification)

Other Work Experience

- Opinion Market Research Ltd: Evaluating bus service in Christchurch, New Zealand.
- WhiteTie Catering, Christchurch, New Zealand: Event Catering
- ProStaff Promotion und Personell, Vienna, Austria: Event Catering

Personal Details

Non-smoker
Interests and activities: Outdoor, swimming
High stress tolerance, can-do, critical, flexible and can work in an international team

References and Annexes

Available on request